# An analytical study of the behavior of composite girder bridges subjected to loads applied parallel to the plane of the slab

by Jagannath Kishanchand Khanna

A thesis submitted to the Graduate Faculty in partial fulfillment of the requirements for the degree of DOCTOR OF PHILOSOPHY in Civil Engineering and Engineering Mechanics
Montana State University


Abstract:
The behavior of composite girder "bridges subjected to loads applied parallel to the plane of the slab was investigated. The finite element method of analysis which treats the slab and the longitudinal girders as an assemblage of plate elements was used. The force displacement relationship for the rectangular plate element was developed with six degrees of freedom, three translations and three rotations.

The series method of substructures is explained for solving a large number of simultaneous equations.

The influence of three kinds of diaphragms, beam, bar and plate diaphragms, on the behavior of the bridge was examined. From the analysis it was noted that the bridge undergoes considerable warping in the absence of diaphragms. The beam diaphragms , whose nodes coincide with the nodes of the slab, do not prevent the distortions of the bridge cross section. The bar and plate diaphragms are of great significance in reducing the transverse deflections of the bridge.

The transverse bending moments resulting from the vertical deflections of the girders are sizeable in the absence of bar or plate diaphragms.

The intermediate diaphragms are seen to have great importance in transferring the load from the loaded exterior girder to the unloaded girders when the loads are applied on the bottom edge of the exterior girder.

# AN ANALYTICAL STUDY OF THE BEHAVIOR OF COMPOSITE GIRDER BRIDGES SUBJECTED TO LOADS APPLIED PARALLEL TO THE PLANE OF THE SLAB

by

JAGANNATH KISHANCHAND KHANNA

A thesis submitted to the Graduate Faculty in partial fulfillment of the requirements for the degree

of

DOCTOR OF PHILOSOPHY

in

Civil Engineering and Engineering Mechanics

Approved:

Head, Major Department

Chairman, Examining Committee

Graduate Dean

MONTANA STATE UNIVERSITY
Bozeman, Montana

August, 1969

To

my wife Kaushal

# ACKNOWLEDGEMENTS

The author is indebted to his major advisor, Dr. Fred F. Videon, for his patient guidance and assistance in the course of research and preparation of the thesis. With his interest in the work, he served as a great source of encouragement.

The author also wishes to express his appreciation to all individuals who offered their personal assistance and helped to make this investigation possible. Professor W. O. Keightley, Mr. Gerald A. Frazier, Mr. Ralph E. Powe, and Mr. Gary J. Hawkins deserve special thanks for their unselfish help.

Acknowledgement is also extended to Mrs. Joan Hall for typing the thesis.

The author is most appreciative of the financial support received from the Montana State University and the National Science Foundation, which made his graduate study possible.

TABLE OF CONTENTS

Chapter Page

# LIST OF FIGURES

# LIST OF TABLES

## ABSTRACT

The behavior of composite girder bridges subjected to loads applied parallel to the plane of the slab was investigated. The finite element method of analysis which treats the slab and the longitudinal girders as an assemblage of plate elements was used. The force displacement relationship for the rectangular plate element was developed with six degrees of freedom, three translations and three rotations.

The series method of substructures is explained for solving a large number of simultaneous equations.

The influence of three kinds of diaphragms, beam, bar and plate diaphragms, on the behavior of the bridge was examined. From the analysis it was noted that the bridge undergoes considerable warping in the absence of diaphragms. The beam diaphragms, whose nodes coincide with the nodes of the slab, do not prevent the distortions of the bridge cross section. The bar and plate diaphragms are of great significance in reducing the transverse deflections of the bridge.

The transverse bending moments resulting from the vertical deflections of the girders are sizeable in the absence of bar or plate diaphragms.

The intermediate diaphragms are seen to have great importance in transferring the load from the loaded exterior girder to the unloaded girders when the loads are applied on the bottom edge of the exterior girder.

# NOTATION

| | |
|---|---|
| $a,b$ | plate dimensions in the x and y directions, respectively |
| $A$ | cross sectional area of bar diaphragms |
| $[A]$ | coordinate transformation matrix relating element displacements to displacements of the overall structure |
| $A_s$ | cross sectional area of eccentric beam diaphragms |
| $c$ | a constant = $(1-\gamma)/2$ |
| $[C]$ | matrix relating dimensionless degrees of freedom with generalized coordinates |
| $C_m$ | moment coefficient |
| $[D]$ | matrix of Hooke's coefficients |
| $E$ | modulus of elasticity |
| $\{f\}$ | displacement field described in terms of generalized coordinates |
| $\{F\}$ | force vector |
| $G$ | modulus of rigidity |
| $I$ | total potential energy |
| $I_x$ | moment of inertia of beam cross section with respect to the reference surface |
| $J$ | St. Venant's torsional constant |
| $[k]$ | element stiffness matrix |
| $[\underline{k}]$ | dimensionless stiffness matrix |
| $[K]$ | stiffness matrix for the overall structure |
| $L$ | span length of a bridge |
| $M_x,M_y$ | moments about x and y axes, respectively |

| | |
|---|---|
| $N_x, N_y$ | axial forces per unit length of plate |
| $\{P\}$ | equivalent nodal forces |
| $\{P(x,y)\}$ | matrix of displacement patterns in cartesian coordinates |
| $\{P(\xi,\eta)\}$ | matrix of displacement patterns in dimensionless coordinates |
| $\{Q\}$ | matrix of forces acting on an element |
| $R_x, R_y, R_z$ | longitudinal, transyerse and yertical reactions, respectively |
| $S_x$ | first moment of the stiffner area with respect to the reference surface |
| $[t]$ | transfer matrix relating dimensionless degrees of freedom $\{\underline{\delta}_i\}$ at a node i of the plate element with dimensional degrees of freedom $\{\delta_i\}$ |
| $[T]$ | strain transfer matrix relating dimensional strains to dimensionless strains |
| $u, v, w$ | displacement patterns in x, y and z directions, respectively |
| $\underline{u}, \underline{v}, \underline{w}$ | displacement patterns in $\xi, \eta$ and z directions, respectively |
| $u_x, v_x, w_x$ | partial derivatives of u, v and w with respect to x |
| $u_\xi, v_\xi, w_\xi$ | partial derivatives of u, y and w with respect to $\xi$ |
| $u_y, v_y, w_y$ | partial derivatives of u, v and w with respect to y |
| $u_\eta, v_\eta, w_\eta$ | partial derivatiyes of u, y and w with respect to $\eta$ |
| $U, V, W$ | translational degrees of freedom |
| $x, y, z$ | cartesian coordinate axes |
| $\{\alpha\}, \{\beta\}$ | generalized coordinates |
| $\{\delta\}$ | nodal degrees of freedom |
| $\{\underline{\delta}\}$ | dimensionless degrees of freedom |
| $\Delta L$ | length of beam element |

| | |
|---|---|
| $\{\varepsilon\}$ | strain vector $(\varepsilon_x, \varepsilon_y, \varepsilon_{xy})$ |
| $\{\underline{\varepsilon}\}$ | dimensionless strain vector $(\varepsilon_\xi, \varepsilon_\eta, \varepsilon_{\xi\eta})$ |
| $\xi, \eta$ | dimensionless coordinate axes |
| $\theta_x, \theta_y, \theta_z$ | rotations about x,y and z axes, respectively |
| $\gamma$ | Poisson's ratio |
| $[\Phi(\xi,\eta)]$ | displacement patterns in terms of degrees of freedom |
| $\{\sigma\}$ | column vector of stresses $(\sigma_x, \sigma_y, \tau_{xy})$ |

# INTRODUCTION

## 1.1 GENERAL

Highway bridges consisting of stiffened steel plate or reinforced concrete slab decks supported by and acting compositely with girders have been used extensively during recent years. These bridges are subjected to loads applied perpendicular and parallel to the plane of the slab. The forces parallel to the plane of the slab include wind loads, earthquake loads and centrifugal forces. These lateral forces are normally ignored in the design of the deck slab and the main girders since their effects are thought to be minor compared to the effects of vertical loads. However, they are considered in the design of diaphragms and other lateral bracing between girders.

Existing composite girder bridges have proved satisfactory in their performance. However, it appears that a detailed analytical study of the spatial behavior of the composite girder bridges subjected to horizontal loads has never been undertaken in the past. The complete three-dimensional analysis of the bridge, therefore, can not be carried out using present day techniques.

A satisfactory analysis of a composite girder system can be accomplished by using the orthotropic plate theory provided the loads are applied vertically. When the girder system is subjected to loads applied parallel to the plane of the slab, the use of the orthotropic plate theory is highly questionable, since this type of loading produces torsion, and causes warping of the cross section.

## 1.2 OBJECT AND SCOPE

The purpose of this investigation is to develop an analytical model that can be used to study the response of composite girder systems subjected to loads applied parallel to the plane of the slab. In addition to studying the effects of these loads on the slab and main girders, it is planned to investigate the effect of various types of diaphragms on the structural behavior and load distribution characteristics of the bridge.

A finite element approach is used to study the behavior of composite girder bridges when subjected to lateral loads. The slab and web of the main girders are treated as an assemblage of plate elements. The force displacement relationship for the rectangular plate element having six degrees of freedom at each node (three translations and three rotations), is developed. Flanges of girders are treated as beams lying in the horizontal plane.

The influence coefficients for the deflections, shears and moments, etc., for composite girder bridges are obtained for the unit horizontal load. The loads are applied at the node points of the top and bottom flanges of the exterior girders. In order to analyze the role of diaphragms and to study the changes in the behavior of the bridges due to the inclusion of the diaphragms, the bridges are solved without diaphragms in one case and with diaphragms at the end sections of the bridges and at an interval of one-quarter span.

The study includes three kinds of diaphragms; beams, bars and plate

diaphragms. The beam diaphragms are treated as an assemblage of beam elements whose nodes coincide with the nodes of the middle plane of the slab. Plate and bar diaphragms are assumed to have nodes which coincide with the nodes of the top and the bottom flanges of the longitudinal girders.

The study also considers two different support conditions for the bridge. In one case the girders of the bridge are pinned at one end and are supported on rollers at the other end, whereas, in the second case both ends of the girders are pinned.

Various other parameters that affect the behavior of bridges, e.g., the relative stiffness of slab and longitudinal girders, number and spacing of longitudinal girders and diaphragms, are not included in the present investigation. Similarly the investigation does not consider the stability analysis of the bridge structures.

## 1.3 BACKGROUND

There is no literature available for analyzing the effects of horizontal loads on the composite girder bridges. A few techniques of analyses for the distribution of the vertical loads to the various longitudinal members forming the bridge are well known.

One method divides the structure into individual and longitudinal and transverse members, each possessing an appropriate flexural and torsional stiffness. For each point of intersection of the members, equations of deflections and slope compatibility are set up and a set of

governing simultaneous differential and/or algebraic equations is solved. Here, one could distinguish between the longitudinal or primary members of the structure from the secondary or transverse members by modifying the stiffness properties of various members. The works of Lightfoot and Sawko (1,2)*, Hendry and Jaegar (3), Hetenyi (4), Pippard and De Waele (5) are examples of the above method.

As is indicated by Davis, et al, (6), Newmark (7) developed a distribution procedure for application to slab on steel I-beams, wherein he assumed negligible shear transfer of longitudinal shear at the beam slab interface. He used the moment distribution method modified to include slab elements to distribute the transverse slab moments and shears. In this technique the flexural rigidity of the girders could be adjusted to compensate for composite action of the slab with the supporting girders.

A more rigorous method of analysis considers a composite beam bridge as an elastically equivalent slab system, an "orthotropic plate", whose structural properties in the two orthogonal directions are uniformly distributed along their length. Analyses of the orthotropic plates are generally based on Huber's (8) theory of anisotropic plates. Such a simplification of the bridge may be justified if (a) the ratios of stiffener spacing to slab boundary dimensions are very small to ensure approximate homogenity of stiffness, (b) flexural and torsional rigidities are independent of the boundary conditions of the slab and the distribution of the load, (c) perfect bond exists between the slab and eccentric stiffeners, and

* Numbers in parentheses refer to references.

(d) there is no warping of the cross section of the bridge structure.

The idea of applying the theory of orthotropic plates to a grid system of a bridge deck by treating it as an idealized plate was proposed by Guyan (9) in 1946. Later, Massonnet (10, 11, 12), Cornelius (13), Pfluger (14, 15), Trenks (16), Glencke (17), and others extended and generalized the use of this method. Pfluger developed a system of three fourth order differential equations in order to include in-plane motions of the plate. Trenks showed that three simultaneous differential equations expressing three components of deformation of the deck plate may be transformed into one differential equation of eighth order. Most of the research published in recent years involves theoretical studies of orthotropic deck plates and deals with mathematical methods for analysing such structures (18 - 24).

A primary drawback of the orthotropic plate method is that the stiffnesses of the slab and beam are to be 'smeared' into an equivalent plate. The flexural and torsional rigidities of the plate can, at best, be approximations and are often difficult to evaluate. Secondly, once the solution of the plate problem is obtained, it is difficult to isolate the moments, shears and displacements for the longitudinal and transverse girders, which are of primary importance.

# FINITE ELEMENT METHOD OF ANALYSIS

## 2.1 GENERAL

In the present investigation the finite element idealization is used as the basic numerical technique to solve a set of differential equations of a continuum with regard to appropriate boundary conditions. Engineering structures built up of bars, beams and plates are generally too complex to be analyzed by the theory of elasticity. The problem becomes tractable if the fundamental conditions of equilibrium and compatibility are expressed in such a manner that the mathematical formulation is given in terms of algebraic equations. The finite element technique is a convenient scheme for obtaining these equations.

The finite element method is very well described in the literature (25,26) and hence only a brief description of the general features of the method are given here. In addition, certain features of the present study which have not been presented before are discussed in detail.

The finite element method is divided into three steps:

Step 1: Structural Idealization:

A structural system is considered as an assemblage of discrete structural elements interconnected at a limited number of node points, usually the corners of the elements. Each element is assumed to have only a finite number of degrees of freedom. The formulation of such a model, referred to as the structural idealization, reduces the infinite degrees of freedom of the continuum to finite degrees of freedom suitable for the

matrix method of analysis. An engineering judgement is vital at this stage since an exact analysis is performed on this substitute structure and hence the results are valid only to the extent the substitute structure represents the original structure.

Step 2: Evaluation of Element Properties:

The force-displacement relationship - stiffness or flexibility matrix - which must be obtained now is the critical phase of the method. An element which has infinite degrees of freedom is restricted to limited degrees of freedom. This in general implies violation of the continuity conditions or the equilibrium conditions or both. Both compatibility and equilibrium conditions are satisfied only under certain special situations, like the case of bending of beams with two degrees of freedom (slope and deflection) at either end. Most of the elements reported in the literature are based on the displacement method (use of stiffness matrix) of analysis and may be subdivided into the following catagories:

(1) Elements satisfying displacement compatibility,
(2) Elements satisfying equilibrium, or
(3) Elements violating both equilibrium and compatibility

(1) Elements satisfying displacement compatibility:

A set of deformation patterns are chosen to define, uniquely the state of displacement within each element. The nodal displacements act as the undetermined parameters. Selection of the displacement patterns which will explicitly specify continuity of deformations and their first derivatives between adjacent elements is difficult. However, elements satisfying continuity of displacements and

their first derivatives and those which satisfy compatibility of displacements only, along the whole interface between adjacent elements are used in the literature with a great success.

Once the displacement patterns are chosen in terms of nodal degrees of freedom, the principle of virtual displacement or the principle of minimum total potential energy is employed to obtain force displacement relationship for the element. Hence the stiffness matrix for the element is obtained.

The process guarantees equilibrium of nodal forces, but does not ensure the stress equilibrium within the element or along the boundaries of the element unless the displacement functions are chosen so that they identically satisfy the differential equation(s) of equilibrium. The elements satisfying the displacement compatibility along the edges of the adjacent elements provide a lower bound to the correct solution. The value of such a bound is not very great since the underestimation of displacements and stresses is true only in an average sense over the entire continuum and is not necessarily true at every point of the continuum. It may be noted that the deformation patterns are invented rather than derived. Great care is required in choosing functions so that the necessary rigid body displacements are satisfied to ensure convergence to the correct solution.

(2) Elements satisfying equilibrium:

In this technique one assumes stress patterns which are

in equilibrium at the outset instead of assuming displacement distribution as in the previous method (27, 28). Now the virtual force approach or the principle of minimum total complementary potential energy is employed to obtain the stiffness matrix of the element. Alternately the displacement distribution, in terms of nodal degrees of freedom, may be derived from the assumed stress distribution and the method of virtual displacement may be employed for the calculation of the stiffness matrix.

The displacement distribution so obtained, in general, violates the compatibility of boundary displacements on adjacent elements. The method gives an over-estimate of the total strain energy and therefore provides an upper bound on the average displacements. Any distribution of strain can be approximated by uniform strains by reducing the element size. Hence, for convergence to the correct solutions it is essential to include stress patterns which produce uniform strain. The method is, in general, more difficult to derive than the previous method.

(3) Elements violating both equilibrium and compatibility:

Here, the displacement pattern is prescribed along the edges of the element in terms of its nodal values in such a way that complete compatibility between adjacent elements is established. The elasticity problem of the element subjected to these boundary displacements is solved, exactly or approximately. If an exact solution is obtained, an element which satisfies both compatibility and equilibrium conditions is obtained. For an approximate solution the complementary strain energy,

defined in terms of the internally equilibrating stress field, may be minimized. This violates the compatibility conditions within the element and the equilibrium conditions are satisfied only approximately on the boundaries. Experience with this technique has indicated good convergence (29).

Step 3: Analysis of the Element Assemblage:

Once the stiffness matrix for each element of the substitute structure is computed in its local coordinate system, it is modified into a global (entire structure) coordinate system. The elements of the modified stiffness matrix are placed in their correct positions in the larger framework of the stiffness of an entire structure. The overlapping terms are superimposed. This process is equivalent to carrying out the matrix multiplication $[A^T]$ $[K][A]$. Where $[A]$ is a coordinate transformation matrix and $[K]$ is a square matrix with the stiffness matrix of each element listed on its main diagonal (26). In practice, the matrix multiplication is seldom carried out since it is time consuming and takes considerable computer core storage.

A necessary criterion of the assembly is that the degrees of freedom for the node of an element be equal to the degrees of freedom of the node of the structure. This may require expansion of the element stiffness matrix by inserting an appropriate number of zeroes. The general process of assembly for these stiffnesses are identical, irrespective of number of nodes an element possesses.

The stiffness matrix for the entire structure is a singular matrix

because the system is free to move as a rigid body when external loads are applied. The order of singularity of the matrix is equal to the number of possible rigid body motions. If the order of singularity is greater than this, then the structure is internally unstable or collapsible. A nonsingular matrix is now obtained by imposing sufficient boundary restraints on the structure.

It may be noted that forces acting on the structure are limited only to the nodes. If any other type of loads are applied to the structure then they must be reduced to "equivalent nodal forces" in the finite element analysis.

After the stiffness matrix for the structure is assembled, the simultaneous linear equations are ready for solution. Any standard method of solution of simultaneous equations may be employed. Certain special techniques may be used to solve a large number of simultaneous equations (see Chapter 3).

## 2.2 FINITE ELEMENT MODEL FOR BRIDGE STRUCTURE

The finite element approach is employed to treat a typical composite floor system (Figure 1) as a three dimensional space structure. The slab and girder elements are treated as an assemblage of rectangular plate elements each of its nodes having six degrees of freedom. Three degrees of freedom describe the transverse bending of the plate element and the remaining

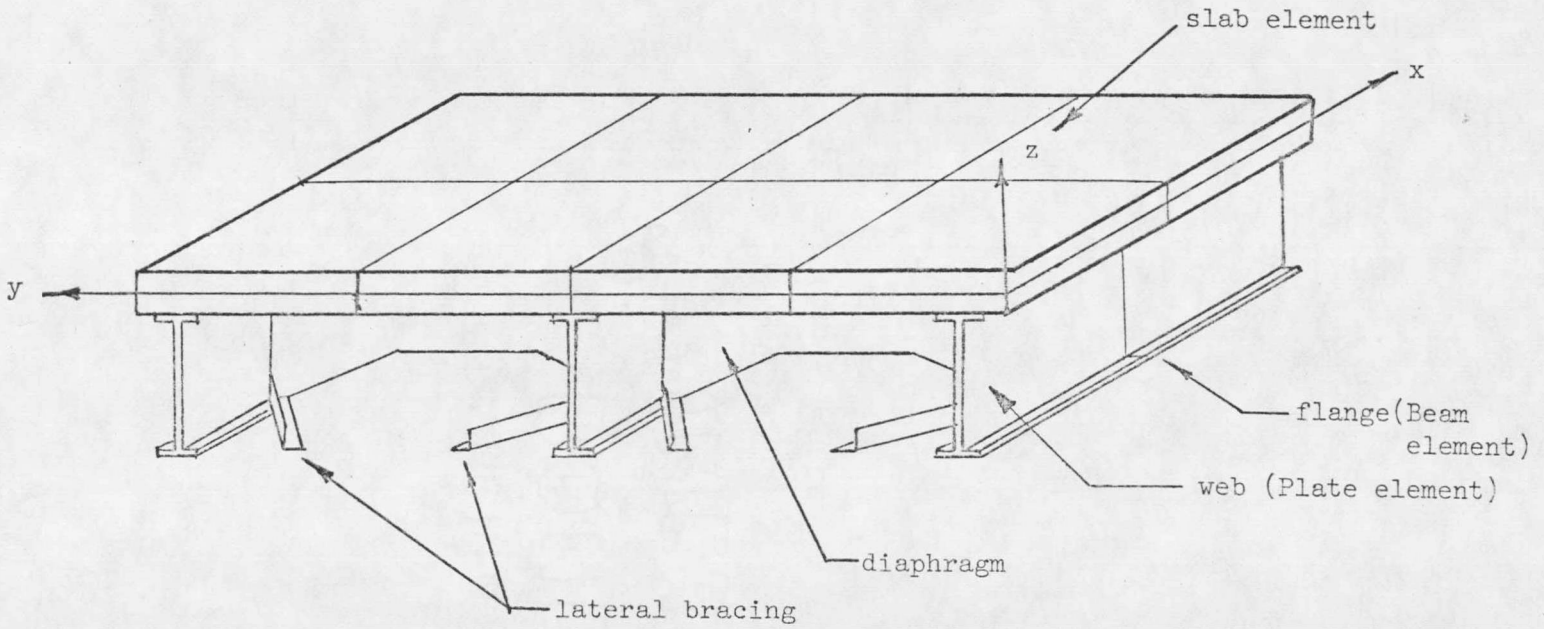


Figure 1: Typical Composite Girder System.

three degrees of freedom describe in-plane deformations of the plate. The flanges of the girders are treated as beams lying in a horizontal plane. Lateral bracing, if any, is treated as bars having only extensional stiffness.

2.2.1 Development of Stiffness Matrices for the Elements.

2.2.1.1 A Plate Element:

For a plate element the in-plane and bending deformations are treated as uncoupled for small deflections, and consequently, elastic properties can be evaluated separately for the in-plane and out-of-plane forces. The stiffness matrices for the two cases; in-plane stretching and transverse bending, are obtained independently, and the stiffness matrix for the total nodal degrees of freedom is obtained simply by combining these stiffnesses.

Consider a plate element ijkl, lying in the x-y plane, as shown in Figure 2. At each node six degrees of freedom are permitted. Three of them are translations U, V and W in the directions of the x, y, and z axes, and three are rotations $\theta_x$, $\theta_y$, and $\theta_z$ about the x, y, and z axes respectively. Positive directions of the rotations are determined by the right-hand screw rule and are shown by vectors directed along these axes.

For the element,

$$\theta_x = w_y$$

$$\theta_y = -w_x$$

and, $\theta_z = (v_x - u_y)/2$

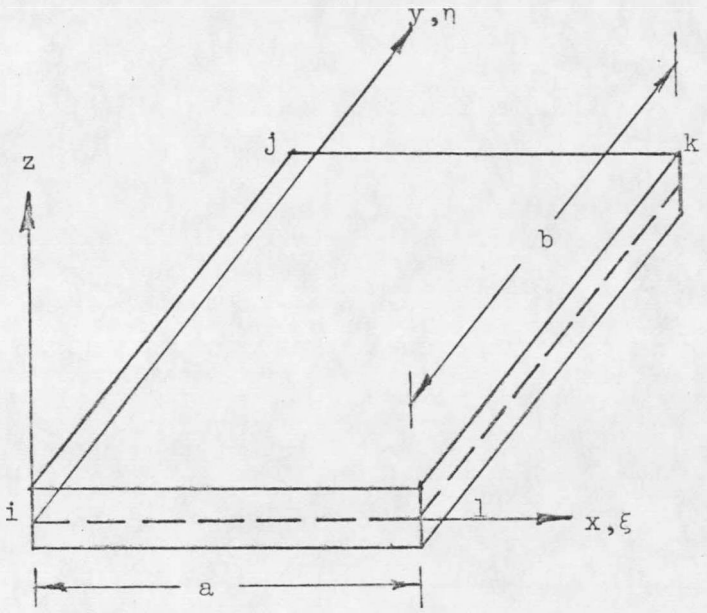


Plate Element

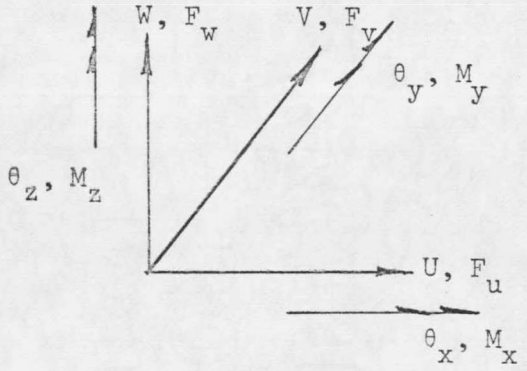


Sign Convention

Figure 2. Plate Element and Coordinate System

where $w_y$ is the partial derivative of transverse deflection w with respect to y, $w_x$ is the partial derivative of w with respect to x, and $v_x$ and $u_y$ are partial derivatives of v and u with respect to x and y, respectively.

Several rectangular plate elements having three degrees of freedom W, $W_x$ and $W_y$ are reported in the literature. Clough (30) has compared some of these elements and has presented a plate bending element which is a "best" element, both in terms of convergence and in terms of approximating true displacements and moments in the plate. The stiffness matrix of this element is used for the transverse bending stiffness of the plate element in the present analysis. The element is based on twelve generalized displacement patterns ($1, x, y, x^2, xy, y^2, x^3, x^2y, xy^2, y^3, x^3y, xy^3$). It is observed that the element satisfies equilibrium and displacement compatibility along the edges of the plate element whereas it does not satisfy the slope continuity along the boundaries.

On the other hand, there is no plane stress element described in the literature with U, V and $\theta_z$ degrees of freedom at its nodes.* In the past, elements with only two degrees of freedom, U and V, have been used. In the case of shell problems, where the third degree of freedom is desired, the corresponding stiffness matrix is obtained by inserting an appropriate number of zeroes into the stiffness matrix (25, p. 126; 31, p. 133). This not only is a misrepresentation of the element

* Triangular plate elements with six degrees of freedom U, V, $\varepsilon_x$, $\varepsilon_y$, $\gamma_{xy}$ and $\theta_z$, and U, V, $U_x$, $U_y$, $V_x$ and $V_y$ at each node are presented in references 32 and 33.

stiffness but it also results in a singular matrix if all the elements should lie in one plane.

Development of a plate element with the above three degrees of freedom is of great engineering importance since it can be used for the case of concentrated moments and for the case of in-plane rotations, which are frequently encountered when two flat plates meet at an angle as in the case of folded plates, or when continuously curved surfaces of shells are approximated by flat plate segments. In folded plates and shells the element is subjected, generally, to both bending and in-plane forces. A detailed derivation of the stiffness matrix for the in-plane stretching of a rectangular plate element is presented.

The general procedure for obtaining the stiffness matrix for an element with assumed displacement patterns - with nodal degrees of freedom as unknown parameters - is described in section 2.1. The method is adopted to obtain the stiffness matrix of the plane stress element in the following two sections.

Section 2.2.1.2 is devoted to the selection of the displacement patterns. In this section the displacement patterns at first are assumed in terms of the generalized coefficients $\{\alpha\}$ and later are related to the nodal degrees of freedom $\{\delta\}$.

In section 2.2.1.3 the principle of the minimum total potential energy is used to compute the stiffness matrix for the plate element for the displacement patterns of section 2.2.1.2.

2.2.1.2 Selection of Displacement Patterns

There are three generalized displacements at each node, two translations and one rotation, and a total of twelve for the element. These twelve nodal displacements establish the boundary conditions for the function which is selected to describe the deformations within the region of the element. This permits the use of a displacement field f(x,y) with twelve generalized coordinates {α}. Since the displacements along the x and y axes are, in general, independent of each other and symmetric in nature, it is desired to select six displacement patterns for u(x,y) and six symmetric displacement patterns to describe the v(x,y) deformation. Polynomial functions are easy to deal with and hence are frequently used in the finite element analysis. In order to choose simple deformation patterns, the functions are restricted to third order polynomials. If all the third order polynomial terms are included then there are twenty generalized coordinates {α}, ten for the u(x,y) displacements and ten for the v(x,y) displacements. The $\theta_z(x,y)$ deformations are computed from the expressions of u(x,y) and v(x,y). (See Equations 2.1 through 2.6.)

$$\{f(x,y)\} = \begin{Bmatrix} u(x,y) \\ v(x,y) \\ \theta_z(x,y) \end{Bmatrix} = [P(x,y)]\ \{\alpha\} \qquad (2.1)$$

where: $[P(x,y)] =$

$$\begin{bmatrix} b & o & \frac{bx}{a} & o & \frac{by}{b} & o & \frac{bxy}{ab} & 0 & \frac{by^2}{b^2} & o & \frac{bx^2}{a^2} & o & \frac{bx^2y}{a^2b} & o & \frac{bxy^2}{ab^2} & \frac{bx^3}{a^3} & o & \frac{by^3}{b3} & o \\ o & a & o & \frac{ay}{b} & o & \frac{ax}{a} & o & \frac{axy}{ab} & o & \frac{ax^2}{a^2} & o & \frac{ay^2}{b^2} & o & \frac{axy^2}{ab^2} & o & o & \frac{ay^3}{b^3} & o & \frac{ax^3}{a^3} \\ o & o & o & o & \frac{-1}{2} & \frac{1}{2} & \frac{-x}{2a} & \frac{y}{2b} & \frac{-y}{b} & \frac{x}{a} & o & o & \frac{-x^2}{2a^2} & \frac{y^2}{2b^2} & \frac{-xy}{ab} & o & o & \frac{-3y^2}{2b^2} & \frac{3x^2}{2a^2} \end{bmatrix}^{*} \quad (2.2)$$

and $\{\alpha\}$ is a vector of generalized coordinates.



* This form of the polynomials is selected in order to obtain a simpler polynomial in dimensionless coordinates.

If $\xi = x/a$ and $\eta = y/b$, then;

$$[P(x,y)] = \begin{bmatrix} b & o & o \\ o & a & o \\ o & o & 1 \end{bmatrix} [\underline{P}(\xi,\eta)] \qquad (2.3)$$

where ;

$$[\underline{P}(\xi,\eta)] = \begin{Bmatrix} \underline{u}\,(\xi,\eta) \\ \underline{v}\,(\xi,\eta) \\ \underline{\theta}_z(\xi,\eta) \end{Bmatrix} = \begin{bmatrix} 1 & 0 & \xi & 0 & \eta & 0 & \xi\eta & 0 & \eta^2 & 0 \\ 0 & 1 & 0 & \eta & 0 & \xi & 0 & \eta\xi & 0 & \xi^2 \\ 0 & 0 & 0 & 0 & \frac{-1}{2} & \frac{1}{2} & \frac{-\xi}{2} & \frac{\eta}{2} & -\eta & \xi \end{bmatrix}$$

$$\begin{bmatrix} \xi^2 & 0 & \xi^2\eta & 0 & \xi\eta^2 & 0 & \xi^3 & 0 & \eta^3 & 0 \\ 0 & \eta^2 & 0 & \eta^2\xi & 0 & \xi^2\eta & 0 & \eta^3 & 0 & \xi^3 \\ 0 & 0 & \frac{-\xi^2}{2} & \frac{\eta^2}{2} & -\xi\eta & \eta\xi & 0 & 0 & \frac{-3\eta^2}{2} & \frac{3\xi^2}{2} \end{bmatrix} \qquad (2.4)$$

and:

a and b are lengths of the element along the x and y axes respectively.

This implies that

$$\begin{Bmatrix} u(x,y) \\ v(x,y) \\ \theta_z(x,y) \end{Bmatrix} = \begin{bmatrix} b & 0 & 0 \\ 0 & a & 0 \\ 0 & 0 & 1 \end{bmatrix} \begin{Bmatrix} \underline{u}(\xi,\eta) \\ \underline{v}(\xi,\eta) \\ \underline{\theta}_z(\xi,\eta) \end{Bmatrix} \qquad (2.5)$$

and that:

$$\{\delta_i\} = \begin{bmatrix} b & 0 & 0 \\ 0 & a & 0 \\ 0 & 0 & 1 \end{bmatrix} \{\underline{\delta}_i\} = [t]\{\underline{\delta}_i\} \qquad (2.6)$$

Where $\{\delta_i\}$ is a column vector of the degrees of freedom at node i, $(U_i, V_i, \theta_{zi})$; $\{\underline{\delta}_i\}$ is a column vector of dimensionless degrees of freedom $(\underline{U}_i, \underline{V}_i, \underline{\theta}_{zi})$ of node i; and the transfer matrix [t] is

$$[t] = \begin{bmatrix} b & 0 & 0 \\ 0 & a & 0 \\ 0 & 0 & 1 \end{bmatrix} \qquad (2.7)$$

In order to relate dimensionless degrees of freedom $\{\underline{\delta}\}$ with generalized coordinates $\{\alpha\}$, the coordinates of nodes i, j, k and l are substituted into the matrix $[\underline{P}(\xi,\eta)]$. It may be observed that columns 3, 11, and 17; 7 and 13; 8 and 14; and columns 4, 12 and 18 are identical in the resulting matrix.* Hence, the polynomial terms corresponding to columns 11, 12, 13, 14, 17 and 18, though they are independent displacement patterns, may be discarded from the definition of the function $\underline{P}(\xi,\eta)$. Hence,

$$[\underline{P}(\xi,\eta)] = \begin{bmatrix} 1 & 0 & \xi & 0 & \eta & 0 & \xi\eta & 0 & \eta^2 & 0 & \xi\eta^2 & 0 & \eta^3 & 0 \\ 0 & 1 & 0 & \eta & 0 & \xi & 0 & \eta\xi & 0 & \xi^2 & 0 & \xi^2\eta & 0 & \xi^3 \\ 0 & 0 & 0 & 0 & \frac{-1}{2} & \frac{1}{2} & \frac{-\xi}{2} & \frac{\eta}{2} & -\eta & \xi & -\xi\eta & \xi\eta & \frac{-3\eta^2}{2} & \frac{3\xi^2}{2} \end{bmatrix} \qquad (2.8)$$

Equation 2.8 contains fourteen polynomial terms to define the displacement field $\{\underline{f}(\xi,\eta)\}$ of the plate element. Seven of the terms define $\underline{u}(\xi,\eta)$ displacements and the remaining seven define $\underline{v}(\xi,\eta)$ displacements.

* see Appendix 1, page 130.

Each element has twelve dimensionless degrees of freedom $\{\delta\}$ and fourteen generalized coordinates $\{\alpha\}$. In order to uniquely relate the generalized coordinates $\{\alpha\}$ with the nodal degrees of freedom $\{\delta\}$, only twelve polynomial terms in the definition of $[\underline{P}(\xi,\eta)]$ are needed. Ideally we are interested in a symmetric and independent set of displacement patterns to define $\underline{u}(\xi,\eta)$ and $\underline{v}(\xi,\eta)$ which gives a 12x12, nonsingular matrix. Therefore, one displacement pattern from each definition of $\underline{u}(\xi,\eta)$ and a corresponding function from the definition of $\underline{v}(\xi,\eta)$ must be discarded. In order to retain simple displacement patterns it is preferred to discard a third order term from the definition of $\underline{u}(\xi,\eta)$ and $\underline{v}(\xi,\eta)$. Realistically, an independent set of symmetric displacement patterns is not available when all second order polynomial terms are retained in the definition of $[\underline{P}(\xi,\eta)]$. This is observed by a careful examination of matrix $[C]$ which relates the dimensionless degrees of freedom $\{\delta\}$ with the generalized coordinates $\{\alpha\}$. The matrix $[C]$ is obtained by substituting the dimensionless coordinates for the nodes i, j, k and l of the element in the matrix $[\underline{P}(\xi,\eta)]$. The 10x10 principle minor of the matrix $[C]$ is nonsingular which indicates linear independence of the first ten vectors of the matrix $[C]$. On the other hand, the 12x12 square matrix obtained by omitting columns eleven and twelve, or by deleting columns thirteen and fourteen, of the matrix $[C]$ is singular. This proves the assertion that an independent symmetric set of functions does not exist when all the second order polynomial terms are retained in the definition of $[\underline{P}(\xi,\eta)]$.

It is also noted that any combination of two vectors, other than those mentioned above, are linearly independent of the first ten vectors. This shows that a set of linearly independent, non-symmetric deformations are available to describe the deformations $\underline{u}(\xi,\eta)$ and $\underline{v}(\xi,\eta)$. Non-symmetry of shape functions implies non-isotropy of the material and hence is of little interest.

Upon examination of other combinations of the fourteen vectors of matrix [C], it is found that among the chosen displacement patterns there is no independent symmetric set available to describe the deformations $\underline{u}(\xi,\eta)$ and $\underline{v}(\xi,\eta)$. Hence, we note that an arbitrary choice of independent displacement patterns is inadequate to guarantee existence of an inverse of the matrix [C] which relates the generalized coordinates $\{\alpha\}$ to the dimensionless degrees of freedom $\{\underline{\delta}\}$.

In order to define a symmetric set of shape functions, an interdependent set of displacement functions is required. This is easily done by retaining the first ten vectors of the matrix $[\underline{P}(\xi,\eta)]$, and by replacing the last four columns by two columns which are linear combinations of columns eleven and twelve and columns thirteen and fourteen respectively. Hence,

$$[\underline{P}(\xi,\eta)] = \begin{bmatrix} 1 & 0 & \xi & 0 & \eta & 0 & \xi\eta & 0 & \eta^2 & 0 & -\xi\eta^2 & -\eta^3 \\ 0 & 1 & 0 & \eta & 0 & \xi & 0 & \eta\xi & 0 & \xi^2 & \xi^2\eta & \xi^3 \\ 0 & 0 & 0 & 0 & \frac{-1}{2} & \frac{1}{2} & \frac{-\xi}{2} & \frac{\eta}{2} & -\eta & \xi & 2\xi\eta & \frac{3}{2}(\xi^2+\eta^2) \end{bmatrix} \tag{2.9}$$

Matrix [C], obtained by substituting the coordinates of nodes i, j, k and l into the matrix $[\underline{P}(\xi,\eta)]$, is easily inverted.

A dimensionless displacement field of the element $\{f(\xi,\eta)\}$, is related to the dimensionless degrees of freedom $\{\underline{\delta}\}$ by:

$$\{\underline{f}(\xi,\eta)\} = \begin{bmatrix} b & 0 & 0 \\ 0 & a & 0 \\ 0 & 0 & 1 \end{bmatrix} [\underline{P}(\xi,\eta)][C^{-1}]\{\underline{\delta}\} \tag{2.10}$$

Equations 2.6 and 2.7 relate the dimensionless degrees of freedom $\{\underline{\delta}\}$ with dimensional degrees of freedom $\{\delta\}$ as:

$$\{\underline{\delta}\} = \begin{bmatrix} [t]^{-1} & 0 & 0 & 0 \\ 0 & [t]^{-1} & 0 & 0 \\ 0 & 0 & [t]^{-1} & 0 \\ 0 & 0 & 0 & [t]^{-1} \end{bmatrix} \{\delta\} \tag{2.11}$$

Substituting Equation 2.11 into Equation 2.10, we obtain the displacement patterns in terms of the nodal degrees of freedom.

$$\{\underline{f}(\xi,\eta)\} = [t][\underline{P}(\xi,\eta)][C^{-1}] \begin{bmatrix} [t]^{-1} & 0 & 0 & 0 \\ 0 & [t]^{-1} & 0 & 0 \\ 0 & 0 & [t]^{-1} & 0 \\ 0 & 0 & 0 & [t]^{-1} \end{bmatrix} \{\delta\} \tag{2.12a}$$

$$= [\Phi(\xi,\eta)]\{\delta\} \tag{2.12b}$$

where:

$$[\Phi(\xi,\eta)] = [t][\underline{P}(\xi,\eta)][C^{-1}]\begin{bmatrix}[t]^{-1} & 0 & 0 & 0\\ 0 & [t]^{-1} & 0 & 0\\ 0 & 0 & [t]^{-1} & 0\\ 0 & 0 & 0 & [t]^{-1}\end{bmatrix} \qquad (2.13)$$

2.2.1.3 Determination of Stiffness for the Plate Element

The total potential energy I of the elastic system in Equation 2.14 is made up of two parts, (a) internal strain energy, and (b) the energy of loads acting at the nodes, or:

$$I = 1/2 \int_v \{\sigma\}^T\{\varepsilon\}dv - \{\delta\}^T\{F\} \qquad (2.14)$$

where:

$\{\varepsilon\}$ = column vector of strains $(\varepsilon_x, \varepsilon_y, \gamma_{xy})$,

$\{\sigma\}$ = column vector of stresses $(\sigma_x, \sigma_y, \tau_{xy})$, and

$\{F\}$ = column vector of nodal forces $(F_{xi}, F_{yi}, F_{\theta zi}\ldots\ldots)$

From the definition of strains:

$$\{\varepsilon\} = \begin{Bmatrix}\varepsilon_x\\ \varepsilon_y\\ \gamma_{xy}\end{Bmatrix} = \begin{bmatrix}\frac{\partial}{\partial x} & 0 & 0\\ 0 & \frac{\partial}{\partial y} & 0\\ \frac{\partial}{\partial y} & \frac{\partial}{\partial x} & 0\end{bmatrix}[P(x,y)] \qquad (2.15a)$$

$$= \begin{bmatrix}\frac{1}{a}\frac{\partial}{\partial \xi} & 0 & 0\\ 0 & \frac{1}{b}\frac{\partial}{\partial \eta} & 0\\ \frac{1}{b}\frac{\partial}{\partial \eta} & \frac{1}{a}\frac{\partial}{\partial \xi} & 0\end{bmatrix}\begin{bmatrix}b & 0 & 0\\ 0 & a & 0\\ 0 & 0 & 1\end{bmatrix}[\underline{P}(\xi,\eta)] \qquad (2.15b)$$

$$= \begin{bmatrix} \frac{b}{a} & 0 & 0 \\ 0 & \frac{a}{b} & 0 \\ 0 & 0 & 1 \end{bmatrix} \begin{bmatrix} \frac{\partial}{\partial \xi} & 0 & 0 \\ 0 & \frac{\partial}{\partial \eta} & 0 \\ \frac{\partial}{\partial \eta} & \frac{\partial}{\partial \xi} & 0 \end{bmatrix} \begin{Bmatrix} \underline{u}(\xi,\eta) \\ \underline{v}(\xi,\eta) \\ \underline{\Theta}_z(\xi,\eta) \end{Bmatrix} \qquad (2.15c)$$

$$= [T]\{\underline{\varepsilon}\}$$

where the strain transfer matrix

$$[T] = \begin{bmatrix} \frac{b}{a} & 0 & 0 \\ 0 & \frac{a}{b} & 0 \\ 0 & 0 & 1 \end{bmatrix} \qquad (2.15d)$$

and the dimensionless strain vector

$$\{\varepsilon\} = \begin{Bmatrix} \underline{u}_\xi \\ \underline{v}_\eta \\ \underline{u}_\eta + \underline{v}_\xi \end{Bmatrix} = [\underline{B}]\{\delta\} \qquad (2.16)$$

The matrix [B] in Equation 2.16 is obtained by proper differentiation of the matrix $[\Phi(\xi,\eta)]$ of Equation 2.13.

From the generalized Hooke's law, the stresses are:

$$\{\sigma\} = [D]\{\varepsilon\} = [D][T]\{\underline{\varepsilon}\} = [D][T][\underline{B}]\{\delta\} \tag{2.17}$$

where:

$$[D] = \frac{E}{1-\gamma^2}\begin{bmatrix} 1 & \gamma & 0 \\ \gamma & 1 & 0 \\ 0 & 0 & \frac{1-\gamma}{2} \end{bmatrix} \tag{2.18}$$

E in Equation 2.18 is the modulus of elasticity, and $\gamma$ is Poisson's ratio for the material.

Substituting Equations 2.15, 2.16 and 2.17 into Equation 2.14 yields:

$$I = \frac{1}{2}\int_v ([D][T][\underline{B}]\{\delta\})^T([T][\underline{B}]\{\delta\})\, dV - \{\delta\}^T\{F\} \tag{2.19a}$$

$$I = \frac{1}{2}\{\delta\}^T[k]\{\delta\} - \{\delta\}^T\{F\} \tag{2.19b}$$

$$\text{where } [k] = \int_v [\underline{B}]^T[T]^T[D][T][\underline{B}]\, dV \tag{2.20}$$

According to the principle of minimum potential energy

$$\frac{\partial I}{\partial(\delta)} = 0$$

Hence: $[k]\{\delta\} - [F] = \{0\}$

or $[F] = [k]\{\delta\}$ (2.21)

By definition, $[k]$ is the desired stiffness matrix.

Exlicit expressions for the stiffness matrix are derived and presented in Appendix 1 along with the stiffness matrix for the

transverse bending of the plate element.

2.2.1.4 Limitations of the Plane Stress Finite Element

The deflection patterns chosen to represent the stretching of the plate do not completely satisfy the displacement continuity between adjacent elements. Continuity is maintained for the u displacement on edges parallel to the x axis and the v displacement on edges parallel to the y axis. The element exactly satisfies the constant strain situation. To verify this property of the element, uniform compression and uniform shear stresses were applied on a single element. The element is pin supported at one corner and is supported on rollers at the other end. The uniform stresses were reduced to equivalent nodal forces and were applied to the nodes of a single element. Plate elements with length to width ratios varying from 1 to 20 were examined. In all cases, nodal deflections were identical to corresponding deflections obtained with the theory of elasticity solutions. When stresses are not uniform, as in the case of a uniform bending stress, the resulting deflections are 6.25% too small. This disagreement indicates that in the case of linear stress distribution, or where stresses vary as a non-linear function, the plate must be taken as an assembly of small elements so that the distributed stress may be approximated by constant stresses.

Since the element correctly represents a uniform stress situation and it incorporates all the rigid body displacements, it is expected that the solution of plane stress problems obtained with the element will converge to the true solution when the element size is diminished. The

exact solutions to plane stress problems with rectangular boundaries are not easily available, and hence comparisons are limited to a cantilever beam loaded at its free end. It may be noted that the cantilever beam problem is not expected to reveal advantages of additional degrees of freedom of the new element, but is designed to show the convergence criterion.

Deflections of the cantilever beam for various mesh sizes are plotted in Figure 3. The figure also shows deflections of the free end when stiffness matrices proposed by Turner, et al (34) and Melosh (35) are used. Melosh's plate element assumes linear displacement patterns, whereas Turner's element is obtained from self equilibrating stress patterns. This element was found to give the best approximation to the cantilever beam problem by Hooley and Hibbert (36).

### 2.2.2 Beam Elements

As was mentioned in section 2.2 longitudinal girders are treated as plates in a vertical plane and their flanges are treated as beams lying in horizontal planes. If transverse beam diaphragms are provided in the bridge, they are treated as eccentric stiffeners which are rigidly connected to the slab. The stiffness matrix for such an eccentric stiffener, with its nodes in the middle plane of the slab, is based on the displacement equations:

$$u(x,y,z) = u(x,y,0) - zw_x$$

$$v(x,y,z) = v(x,y,0) - zw_y$$

where $u(x,y,0)$ and $v(x,y,0)$ are displacements of the reference surface

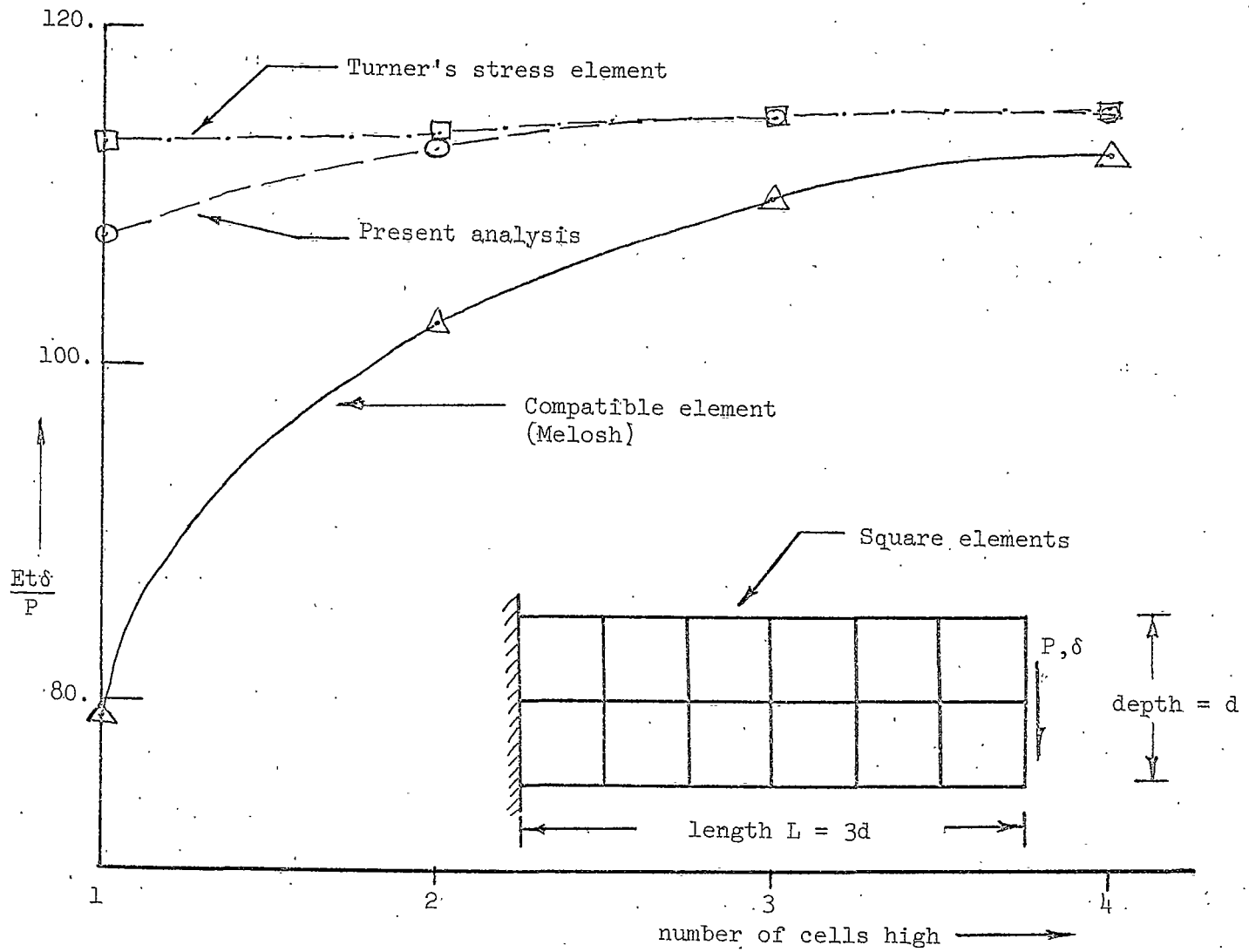


Figure 3. Convergence of finite element method of analysis.

along the x and y axes. These displacements are referred to as the u and v displacements.

If the beam lies entirely in the y-z plane, as is the case with transverse diaphragms, its resistance to motion in the x direction is completely ignored. The displacements in the y and z directions are assumed to be:

$$\begin{Bmatrix} v \\ w \end{Bmatrix} = \begin{bmatrix} 1 & y & 0 & 0 & 0 & 0 \\ 0 & 0 & 1 & y & y^2 & y^3 \end{bmatrix} \{\beta\} \qquad (2.23)$$

Proceeding as in the case of the rectangular plate in extension, the generalized coefficients $\{\beta\}$ are related to degrees of freedom V, W, and $W_y(=\theta_x)$ of the beam element by:

$$\{\beta\} = [C^{-1}]\{\delta\} \qquad (2.24)$$

where $[C]$ is 6x6 matrix of nodal coordinates.

The displacements in Equation 2.23 are represented in terms of the degrees of freedom $\{\delta\}$ of the beam element by:

$$\begin{Bmatrix} v \\ w \end{Bmatrix} = \begin{bmatrix} 1 & y & 0 & 0 & 0 & 0 \\ 0 & 0 & 1 & y & y^2 & y^3 \end{bmatrix} [C^{-1}]\{\delta\} \qquad (2.25)$$

Therefore, the strain and stress vectors are given by:

$$\{\varepsilon_y\} = v_y - zw_{yy} = (0\ 1\ 0\ 0\ -2z\ -6zy)\ [C^{-1}]\ \{\delta\} \qquad (2.26)$$

and

$$\{\sigma\} = E\{\varepsilon_y\} \qquad (2.27)$$

The principle of minimum total potential energy gives the desired matrix equation:

$$\begin{Bmatrix} F_{v1} \\ F_{w1} \\ F_{\theta x1} \\ F_{v2} \\ F_{w2} \\ F_{\theta x2} \end{Bmatrix} = E^* \begin{bmatrix} \frac{A_s}{\Delta L} & & & & & \\ 0 & \frac{12I_x}{\Delta L^3} & & \text{Symmetric} & & \\ -\frac{S_x}{\Delta L} & -\frac{6I_x}{\Delta L^2} & \frac{4I_x}{\Delta L} & & & \\ -\frac{A_s}{\Delta L} & 0 & \frac{S_x}{\Delta L} & \frac{A_s}{\Delta L} & & \\ 0 & -\frac{12I_x}{\Delta L^3} & \frac{6I_x}{\Delta L^2} & 0 & \frac{12I_x}{\Delta L^3} & \\ \frac{S_x}{\Delta L} & -\frac{6I_x}{\Delta L^2} & \frac{2I_x}{\Delta L} & -\frac{S_x}{\Delta L} & \frac{6I_x}{\Delta L^2} & \frac{4I_x}{\Delta L^2} \end{bmatrix} \begin{Bmatrix} v_1 \\ w_1 \\ \theta_{x1} \\ v_2 \\ w_2 \\ \theta_{x2} \end{Bmatrix} \qquad (2.28)$$

In the above equations, $A_s$ is the cross sectional area of the stiffner, $S_x$ is the first moment of the stiffner area with respect to the reference surface, and $I_x$ is the moment of inertia of the stiffner with respect to the reference surface.

In order to consider torsional resistance of the stiffner, extra degrees of freedom $\theta_y$ are introduced at both ends of the beam element. Assuming the angle of twist varies linearly along the length of the element, the twisting moments, $F_{\theta_y}$, are related to the degree of freedom $\theta_y$ by:

$$\begin{Bmatrix} F_{\theta_{y1}} \\ F_{\theta_{y2}} \end{Bmatrix} = E \begin{bmatrix} \gamma & -\gamma \\ -\gamma & \gamma \end{bmatrix} \begin{Bmatrix} \theta_{y1} \\ \theta_{y2} \end{Bmatrix} \qquad (2.29)$$

where $\gamma = GJ/E\Delta L$; G is the shear modulus, $J = \sum^{n} \frac{1}{3} bt^3$, and $\Delta L$ is the length of the beam element.

The torsional stiffness may be combined with the stiffness matrix of Equation 2.24 to obtain a stiffness matrix for the beam element having four degrees of freedom V, W, $\theta_x$ and $\theta_y$ at its nodes. The matrix is shown in Appendix 1. If the reference surface is assumed to pass through the neutral axis of the beam element then the stiffness matrix of the beam element may be reduced to a more familiar form by substituting $S_x = 0$ in the stiffness matrix.

### 2.2.3 Bar Elements

Bars or axial force members are used in the bridge as lateral

bracing or as diaphragms. The stiffness matrix of the bar element is obtained in local coordinates simply by assuming linear displacement patterns. If the direction of the axis of the bar is denoted by $\bar{x}$ and the displacements and forces in this direction by $\bar{u}$ and $\bar{F}_u$ respectively, then the stiffness matrix for a bar element of length $\Delta L$ is given by:

$$\begin{Bmatrix} \bar{F}_{u1} \\ \bar{F}_{u2} \end{Bmatrix} = \frac{A\,E}{\Delta\,L} \begin{bmatrix} 1 & -1 \\ -1 & 1 \end{bmatrix} \begin{Bmatrix} \bar{U}_1 \\ \bar{U}_2 \end{Bmatrix} \tag{2.30}$$

where A is the area of cross section of the bar element.

## 2.3 EQUIVALENT NODAL FORCES

In the finite element analysis of the structure, loads are restricted to the nodes, whereas the orientation of the actual loads on the structure is arbitrary, e.g., truck loads on a bridge. Or, the loads are distributed over the structure as is the case with the dead load of the structure. In the finite element analysis one needs to replace the actual loads acting on the structure by the equivalent nodal forces. This replacement is easily done by equating the virtual work of the two systems:

$$\delta W = \int_s \delta\{f\}^T[Q]ds = \delta\{\delta\}^T\{P\}_{equivalent} \tag{2.31}$$

where $\delta\{f\}$ denotes the virtual displacement of the surface s and [Q] is the matrix of the forces acting on the element, and $\delta\{\delta\}$ is the virtual displacements for the nodal degrees of freedom.

In Equation 2.12, $\{f\} = [\Phi]\{\delta\}$, hence:

$$\delta\{f\} = [\Phi]\delta\{\delta\} \tag{2.32}$$

Substituting Equation 2.32 in Equation 2.31,

$$\delta\{\delta\}^T \int_S [\Phi]^T[Q]ds = \delta\{\delta\}^T\{P\}_{equivalent} \tag{2.33}$$

Since virtual displacements $\delta\{\delta\}$ are arbitrary

$$\{P\}_{equivalent} = \int_S [\Phi]^T[Q]ds \tag{2.34}$$

To illustrate the method, equivalent nodal forces for the cases of uniform compression and uniform shear stress acting on the plane stress element of the previous section are computed. When the compressive stresses are acting on the edges parallel to y axis, the integration in Equation 2.34 is carried out only along these edges. The vector [Q] of the applied loads is represented by two components, $Col^n(1,0,0)$ along x = 0 and $Col^n(-1,0,0)$ at x = a. On integration Equation 2.34 yields the equivalent nodal forces {P} of Equation 2.35.

$$\{P\}_{\text{compression}} = \begin{Bmatrix} \frac{b}{2} \\ 0 \\ -\frac{b^2}{12} \\ \frac{b}{2} \\ 0 \\ \frac{b^2}{12} \\ -\frac{b}{2} \\ 0 \\ -\frac{b^2}{12} \\ -\frac{b}{2} \\ 0 \\ \frac{b^2}{12} \end{Bmatrix} \qquad (2.35)$$

Similarly, the equivalent nodal forces for the cases of uniform shear stresses and uniform bending stresses acting on edges parallel to y axis are obtained as shown in Equations 2.36 and 2.37, respectively.

$$\{P\}_{shear} = \begin{Bmatrix} -\frac{a}{2} \\ -\frac{b}{2} \\ 0 \\ \hline \frac{a}{2} \\ -\frac{b}{2} \\ 0 \\ \hline \frac{a}{2} \\ \frac{b}{2} \\ 0 \\ \hline -\frac{a}{2} \\ \frac{b}{2} \\ 0 \end{Bmatrix} \tag{2.36}$$

and

$$\{P\}_{\text{bending}} = \begin{Bmatrix} \frac{-b}{6} \\ 0 \\ 0 \\ \hline \frac{b}{6} \\ 0 \\ 0 \\ \hline \frac{-b}{6} \\ 0 \\ 0 \\ \hline \frac{b}{6} \\ 0 \\ 0 \end{Bmatrix} \qquad (2.37)$$

# COMPARISONS WITH EXISTING SOLUTIONS

## 3.1 INTRODUCTION

The displacement method of analysis when applied to the analysis of a structure composed of many elements, results in a large number of simultaneous algebraic equations. The conventional techniques adopted for the solution of these equations may cause computational difficulties or may even prove impossible when the order of the matrix exceeds the capacity of the digital computer.

In order to efficiently solve these equations on the computer, advantage must be taken of a high proportion of zero elements in the stiffness matrix. With careful numbering of the nodes, the stiffness matrix of the structure may be obtained so that all the non zero terms are located in a reasonably narrow diagonal band. The band width of the matrix is minimized when the nodes are numbered such that the difference between any two connected node numbers is a minimum. Several papers which deal with the banded form of the matrix have reported considerable economies, both in computing time and computer core storage (37, 38, 39, 40, 41).

Alternately, the structure under consideration may be partitioned into a number of substructures, and the boundaries of the substructures may be specified arbitrarily. If the stiffness matrices for the substructures are determined, then each substructure can be treated as a complex structural element and the displacement method of analysis can be formulated for the partitioned structure. In other words, the idea of a

substructure is nothing more than a generalization of a structural member. Here the substructure is treated as a basic "building block" (42, 43, 44, 45). Such a physical idealization has a mathematical counterpart in the form of partitioned matrices.

The complexity of the interactions between substructures depends primarily upon the manner in which the structure is divided. Moreover, the choice of the scheme for the solution of the resulting matrix equation is related to the layout of substructures. The method of series elimination is the simplest method among the various available techniques of subdivision of the structure. The method is explained briefly in the following section.

## 3.2 SERIES ELIMINATION METHOD OF SUBSTRUCTURE

When the structure is subdivided into 'n' substructures as shown in Figure 4(a), the stiffness matrix [K] for the structure may be partitioned into a tri-diagonal band matrix, as given by:

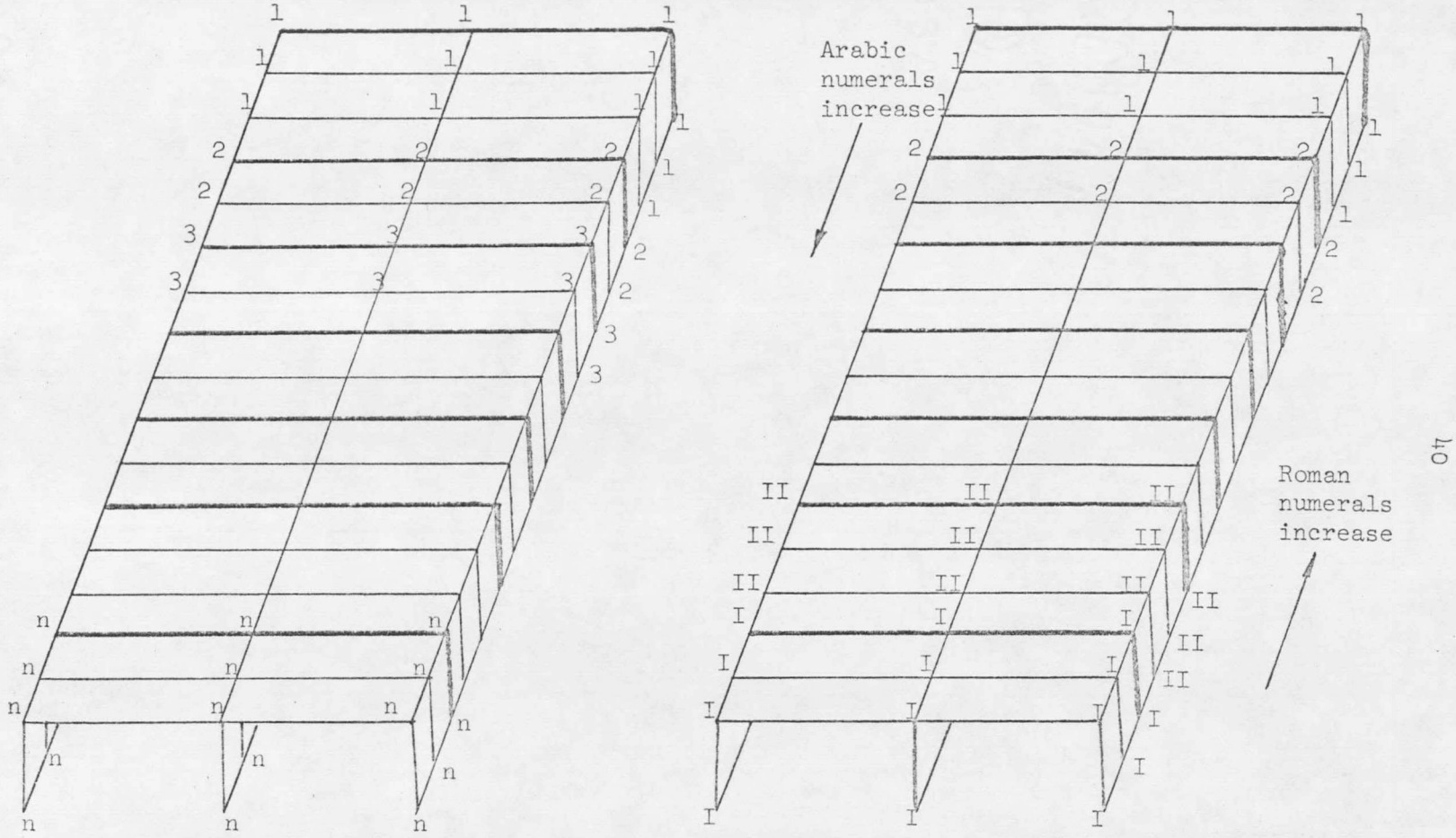


Figure 4. Division of structure into n substructures.

$$
[K]=\begin{bmatrix}
[k]_{11} & [k]_{12} & & & & & & \\
[k]_{21} & [k]_{22} & [k]_{23} & & & & & \\
 & [k]_{32} & [k]_{33} & [k]_{34} & & & & \\
 & & & & & & & \\
 & & & & [k]_{j-1,j} & [k]_{j,j} & [k]_{j,j+1} & \\
 & & & & & & & \\
 & & & & & & [k]_{n-1,n} & [k]_{n,n}
\end{bmatrix}
\qquad (3.1)
$$

Each element $[k]_{j,j}$, in Equation 3.1 corresponds to the stiffness matrix of all nodes of the substructure j, and the matrices $[k]_{j-1,j}$ and $[k]_{j,j+1}$ are the coupling matrices.

One must invert matrix [K] in order to compute the displacements $[\delta]$ for the structure when the nodal forces [F] are applied, or, one must take advantage of the tri-diagonal form of the matrix [K] and set up a recursion relation.

In order to establish the recursion relation for the series elimination, matrices $[\delta]$ and [F] are subdivided as in Equation 3.2.

$$\begin{bmatrix} [F]_1 \\ [F]_2 \\ \\ \\ [F]_n \end{bmatrix} = \begin{bmatrix} [k]_{11} & [k]_{12} & & & & \\ [k]_{21} & [k]_{22} & [k]_{23} & & & \\ & [k]_{32} & [k]_{33} & [k]_{34} & & \\ & & & & & \\ & & & & [k]_{n-1,n} & [k]_{n,n} \end{bmatrix} \begin{bmatrix} [\delta]_1 \\ [\delta]_2 \\ \\ \\ [\delta]_n \end{bmatrix} \qquad (3.2)$$

In Equation 3.2, $\{F\}_j$ and $\{\delta\}_j$ refer, respectively, to the forces and displacements at the nodes of substructure j.

Equation 3.2 may be expanded to 'n' matrix equations. The first and second of these equations are:

$$[k]_{11}\ [\delta]_1 + [k]_{12}\ [\delta]_2 = [F]_1 \text{ , and} \qquad (3.3)$$

$$[k]_{21}\ [\delta]_1 + [k]_{22}\ [\delta]_2 + [k]_{23}\ [\delta]_3 = [F]_2 \qquad (3.4)$$

From Equation 3.3,

$$[\delta]_1 = -[k]_{11}^{-1} \left[ [k]_{12}\ [\delta]_2 - [F]_1 \right] \qquad (3.5)$$

Substituting this expression for $[\delta]_1$ into equation 3.4:

$$[k]^*_{22}\ [\delta]_2 + [k]_{23}\ [\delta]_3 = [F]^*_2 \qquad (3.6)$$

where:

$$[k]^*_{22} = [k]_{22} - [k]_{21}\ [k]_{11}^{-1}\ [k]_{12} \text{ , and} \qquad (3.7)$$

$$[F]^*_2 = [F]_2 - [k]_{21}\ [k]_{11}^{-1}\ [F]_1 \qquad (3.8)$$

From Equation 3.6:

$$[\delta]_2 = -[k]^{*-1}_{22} \left[ [k]_{23} [\delta]_3 - [F]^{*}_2 \right] \qquad (3\text{-}9)$$

The form of Equation 3.9 is identical to the form of Equation 3.5.

The third of the matrix Equations, 3.2, may be written:

$$[F]_3 = [k]_{32} [\delta]_2 + [k]_{33} [\delta]_3 + [k]_{34} [\delta]_4 \qquad (3.10)$$

Equations 3.6 and 3.10 form a pair of equations which are identical in form to the first pair of Equations 3.3 and 3.4. Operating on this pair, just as on the first pair, yields:

$$[k]^{*}_{33} [\delta]_3 + [k]_{34} [\delta]_4 = [F]^{*}_3 \qquad (3\text{-}11)$$

where:

$$[k]^{*}_{33} = [k]_{33} - [k]_{32} [k]^{*-1}_{22} [k]_{23} \text{ , and} \qquad (3\text{-}12)$$

$$[F]^{*}_3 = [F]_3 - [k]_{32} [k]^{*-1}_{22} [F]_2 \qquad (3\text{-}13)$$

Equation 3.11 yields:

$$[\delta]_3 = -[k]^{*-1}_{33} \left[ [k]_{34} [\delta]_4 - [F]^{*}_3 \right] \qquad (3\text{-}14)$$

One may now write the fourth of the matrix Equations 3.2. This equation and Equation 3.11 will form a third pair of equations. This pair of equations is similar in form to the first and second pair. Proceeding as before one can write:

$$[k]^{*}_{44} [\delta]_4 + [k]_{45} [\delta]_5 = [F]^{*}_4 \qquad (3\text{-}15)$$

where: $$[k]^{*}_{44} = [k]_{44} - [k]_{43}[k]^{*-1}_{33}[k]_{34}, \text{ and} \tag{3.16}$$

$$[F]^{*}_{4} = [F]_{4} - [k]_{43}[k]^{*-1}_{33}[F]_{3} \tag{3.17}$$

Proceeding in this manner, the general recursion relation is:

$$[k]^{*}_{j,j}[\delta]_{j} + [k]_{j,j+1}[\delta]_{j+1} = [F]^{*}_{j} \tag{3.18}$$

where:

$$[k]^{*}_{j,j} = [k]_{j,j} - [k]_{j,j-1}[k]^{*-1}_{j-1,j-1}[k]_{j-1,j}, \text{ and} \tag{3.19}$$

$$[F]^{*}_{j} = [F]_{j} - [k]_{j,j-1}[k]^{*-1}_{j-1,j-1}[F]_{j-1} \tag{3.20}$$

From Equation 3.18:

$$[\delta]_{j} = -[k]^{*-1}_{j,j}\left[[k]_{j,j+1}[\delta]_{j+1} - [F]^{*}_{j}\right] \tag{3.21}$$

The process is continued until the last pair of Equations, 3.22 and 3.23, are obtained:

$$[k]^{*}_{n-1,n-1}[\delta]_{n-1} + [k]_{n-1,n}[\delta]_{n} = [F]^{*}_{n-1} \tag{3.22}$$

$$[k]_{n-1,n}[\delta]_{n-1} + [k]_{n,n}[\delta]_{n} = [F]_{n} \tag{3.23}$$

From this pair of equations,

$$[\delta]_{n} = [k]^{*-1}_{n,n}[F]_{n} \tag{3.24}$$

where:

$$[k]^{*}_{n,n} = [k]_{n,n} - [k]_{n,n-1}[k]^{*-1}_{n-1,n-1}[k]_{n-1,n}, \text{ and} \tag{3.25}$$

$$[F]^{*}_{n} = [F]_{n} - [k]_{n,n-1} [k]^{*-1}_{n-1,n-1} [F]_{n-1} \qquad (3.26)$$

Once the deflections $[\delta]_n$ of the last substructure are obtained, the deflections $[\delta]_{n-1}$ for the preceding structure are obtained from Equation 3.21 by substituting $j = n-1$. This process is repeated until the deflections $[\delta]_1$ for the first substructure are obtained.

The process just described computes the deflections of one end and then computes the deflections of the entire structure by using the recursion relation of Equation 3.21. Because of the large number of computations involved in the process it is suspected that a considerable loss in accuracy may result in the deflections of the structure. The error in computations may be reduced by first calculating the deflections of the midsection, and then, relating the deflections of the remaining structure with these deflections. In order to derive the recursion relations for this case, the substructures are numbered as shown in Figure 4(b). The resulting matrix equations are expressed by:

$$\begin{bmatrix} [F]_1 \\ [F]_2 \\ \\ [F]_C \\ \\ [F]_{II} \\ [F]_I \end{bmatrix} = \begin{bmatrix} [k]_{1,1} & [k]_{1,2} & & & & & \\ [k]_{2,1} & [k]_{2,2} & [k]_{2,3} & & & & \\ & & [k]_{C,C-1} & [k]_{C,C} & [k]_{C,C-I} & & \\ & & & [k]_{II,III} & [k]_{II,II} & [k]_{II,I} & \\ & & & & [k]_{I,II} & [k]_{I,I} \end{bmatrix} \begin{bmatrix} [\delta]_1 \\ [\delta]_2 \\ \\ [\delta]_C \\ \\ [\delta]_{II} \\ [\delta]_I \end{bmatrix} \tag{3.27}$$

Proceding as before, one can write the recursion relations Equations 3.18 through 3.21. The index j stands for the $j^{th}$ substructure counted from either end. When j = C-1 (where C is the index of the central substructure), Equation 3.21 becomes;

$$[\delta]_{C-1} = - \overset{*-1}{[k]}_{C-1,C-1} \left[ [k]_{C-1,C} \; [\delta]_C - \overset{*}{[F]}_C \right] \tag{3.28}$$

where:

$$\overset{*}{[F]}_C = [F]_C - [k]_{C,C-1} \; \overset{*-1}{[k]}_{C-1,C-1} \; [F]_{C-1} \tag{3.29}$$

Similarly, when j = C-I, Equation 3.21 becomes:

$$[\delta]_{C-I} = -\overset{**-1}{[k]}_{C-I,C-I} \left[ [k]_{C-I,C} \; [\delta]_C - \overset{**}{[F]}_C \right] \tag{3.30}$$

where:

$$\overset{**}{[F]}_C = [F]_C - [k]_{C,C-I} \; \overset{**-1}{[k]}_{C-I,C-I} \; [F]_{C-I} \tag{3.31}$$

Double stars on the matrices signify that the recursion relation is carried out from the front end, with Roman numerals.

The matrix equation for the central substructure may now be written from Equation 3.2 as:

$$[F]_C = [k]_{C,C-1}\,[\delta]_{C-1} + [k]_{C,C}[\delta]_C + [k]_{C,C-I}\,[\delta]_{C-I} \qquad (3.32)$$

Substituting Equations 3.28 through 3.31 in Equation 3.32:

$$[F]^{***}_C = [k]^{*}_{C,C}[\delta]_C \qquad (3.33)$$

where:

$$[k]^{*}_{C,C} = [k]_{C,C} - [k]_{C,C-1}\,[k]^{*-1}_{C-1,C-1}\,[k]_{C-1,C} - [k]_{C,C-I}\,[k]^{**-1}_{C-I,C-I}\,[k]_{C-I,C} \qquad (3.34)$$

and

$$[F]^{***}_C = [F]_C - [k]_{C,C-1}\,[k]^{*-1}_{C-1,C-1}\,[F]^{*}_C - [k]_{C,C-I}\,[k]^{**-1}_{C-I,C-I}\,[F]^{**}_C \qquad (3.35)$$

After the deflections $[\delta]_C$ are obtained from equation 3.33, the deflections for the remaining structures are obtained by successive applications of the recursion relations of Equations 3.18 to 3.21.

The recursion process requires the inversion of matrices whose largest order is equal to the order of the largest matrix $[k]_{j,j}$. This enables the programmer to conserve the computer core storage, provided he uses the auxiliary storage units for the large blocks of information pertaining to individual substructures. Hence, a large structure may now be analyzed. When auxiliary storage units are used in the program, the benefits derived from a large capacity are partially offset by an increase in computer time. This loss of efficiency is due to the fact that access time is typically much greater for auxiliary storage than for the core

storage. It may, however, be noted that the time of solution varies as a linear function of the number of substructures in the structure, rather than as the cube of the number of unknown deflections $\{\delta\}$, as is the case in ordinary techniques for solving equations.

## 3.3 VERIFICATION OF COMPUTER CODE

A computer program is written to analyze a structure composed of plate, beam and bar elements. The program utilizes the series method of substructures described in the previous section. It is used for the analysis of the bridge structures which are discussed later.

The logic of the program is verified with the cantilever beam problem presented in the second chapter. The cantilever beam problem was solved several times. Each time the beam was divided into different substructures and the scheme of numbering the node points was changed. The deflections of the beam were found identical in each case. For each element nodal forces were computed from the known deflections. The forces acting at each node were then superimposed for equilibrium checks of the nodal forces.

The cantilever beam lies entirely in one plane and is made up only of plate elements. Hence, it does not check certain aspects of the program. Therefore, the program is also verified with a bridge supported on two longitudinal girders. The computed deflections of all the nodes of the bridge were identical for the various combinations of substructures (Figure 5). The equilibrium conditions were also checked at each node of

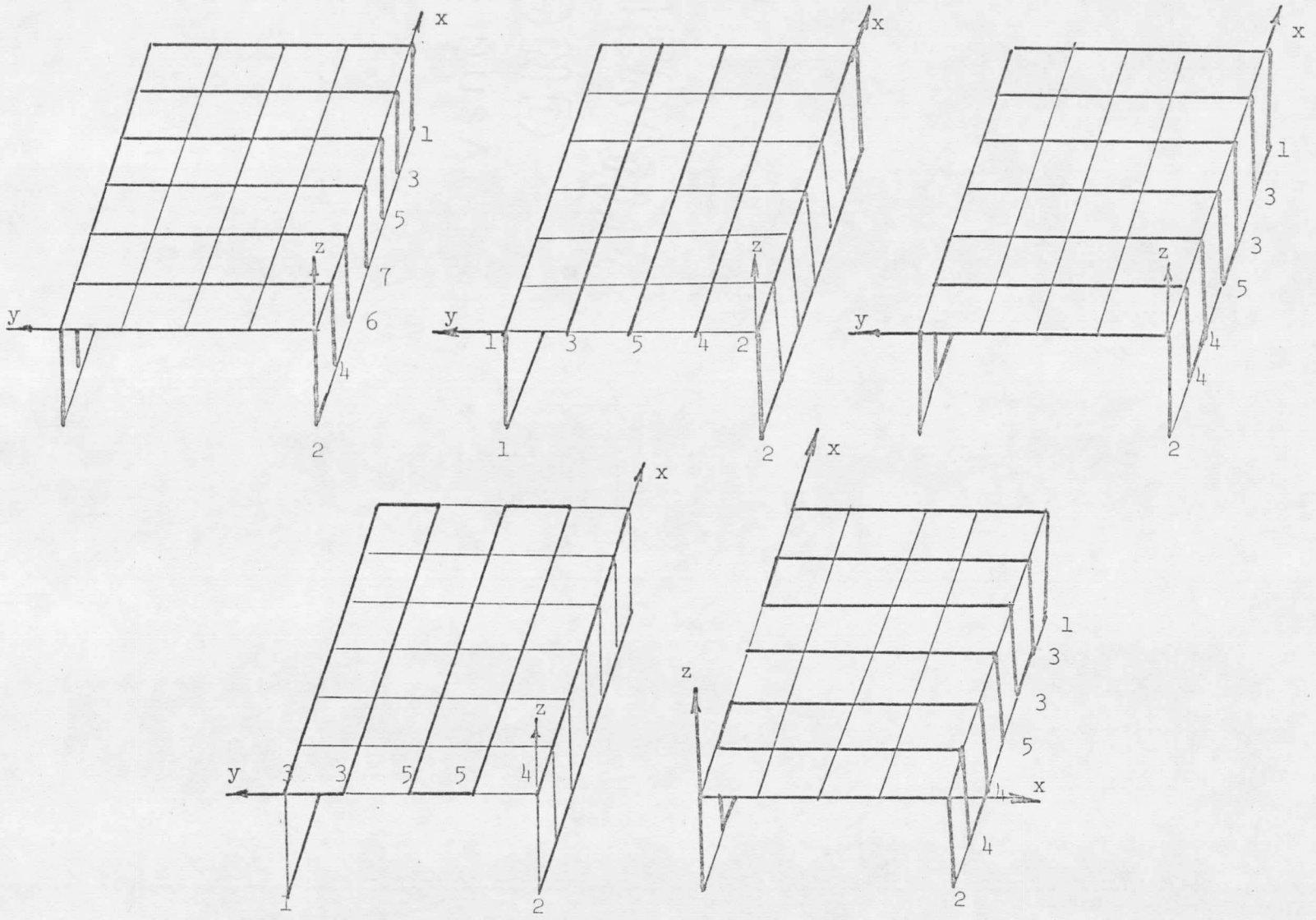


Figure 5. Structure divided into different substructures.

the bridge. The bridge was also solved with axial diaphragms at its supports. The deflections of the various nodes due to applied loads were identical when the structure was subdivided into two different substructures.

## 3.4 COMPARISONS WITH EXISTING SOLUTIONS

The applications of the finite element method of analysis are varied. The method was recently applied to composite I-beam bridges (46). The literature on the finite element method is full of evaluations of the method in comparison to other methods of solution. The evaluations, which are based on comparisons with exact solutions for simple problems and with the experimental results for the more complex problems, have proved a great success of the method. Therefore, in the present study of the bridge behavior under the action of horizontal loads, no attempt is made to justify the use of the method. However, certain comparisons are made to investigate the validity of the method and to illustrate the differences in solutions resulting from the various assumptions made in formulating the analytical models and other approximate methods of solution.

Comparisons are made for vertical loads on three composite I-beam bridges of different span lengths and girder sizes. All the bridges are solved by the finite element method by Gustafson (46). In his model, plate elements have only five degrees of freedom U, V, W, $\theta_x$, and $\theta_y$; and the longitudinal and transverse girders are treated as beam elements. The stiffness of the beam elements is computed by assuming the nodes of the beam elements to coincide with the neutral surface of the slab.

The first bridge studied is a five girder bridge supported over a span of sixty feet (Figure 6). The bridge was solved by Vitols, Clifton and Au by the orthotropic plate theory in order to compare their more accurate treatment of the eccentric stiffners with the conventional technique (19).

In the present analysis the slab of the bridge is represented by a mesh of sixteen longitudinal by ten transverse rectangular plate elements of equal size. Each element of the slab has six degrees of freedom; U, V, W, $\theta_x$, $\theta_y$, and $\theta_z$. The webs of the longitudinal girders are treated as plate elements and their flanges are treated as beams lying in horizontal planes.

Table I gives a comparison of the present investigation for the midspan loading on the girders with the orthotropic plate analysis of Vitols, Clifton and Au, and with the finite element analysis of Gustafson. It also presents moment coefficients for the loads at the quarter span and at three-quarter span of the bridge. The data in Table I shows a somewhat different distribution of load compared to the orthotropic plate theory and Gustafson's finite element model.

It is observed that the differences in the midspan moments between the orthotropic plate analysis and Gustafson's model are greatest when the exterior girder A is loaded. They reduce when girder B is loaded and are a minimum when girder C is loaded. In the present analysis, the moments carried by the interior girders B and C, when the vertical loads are

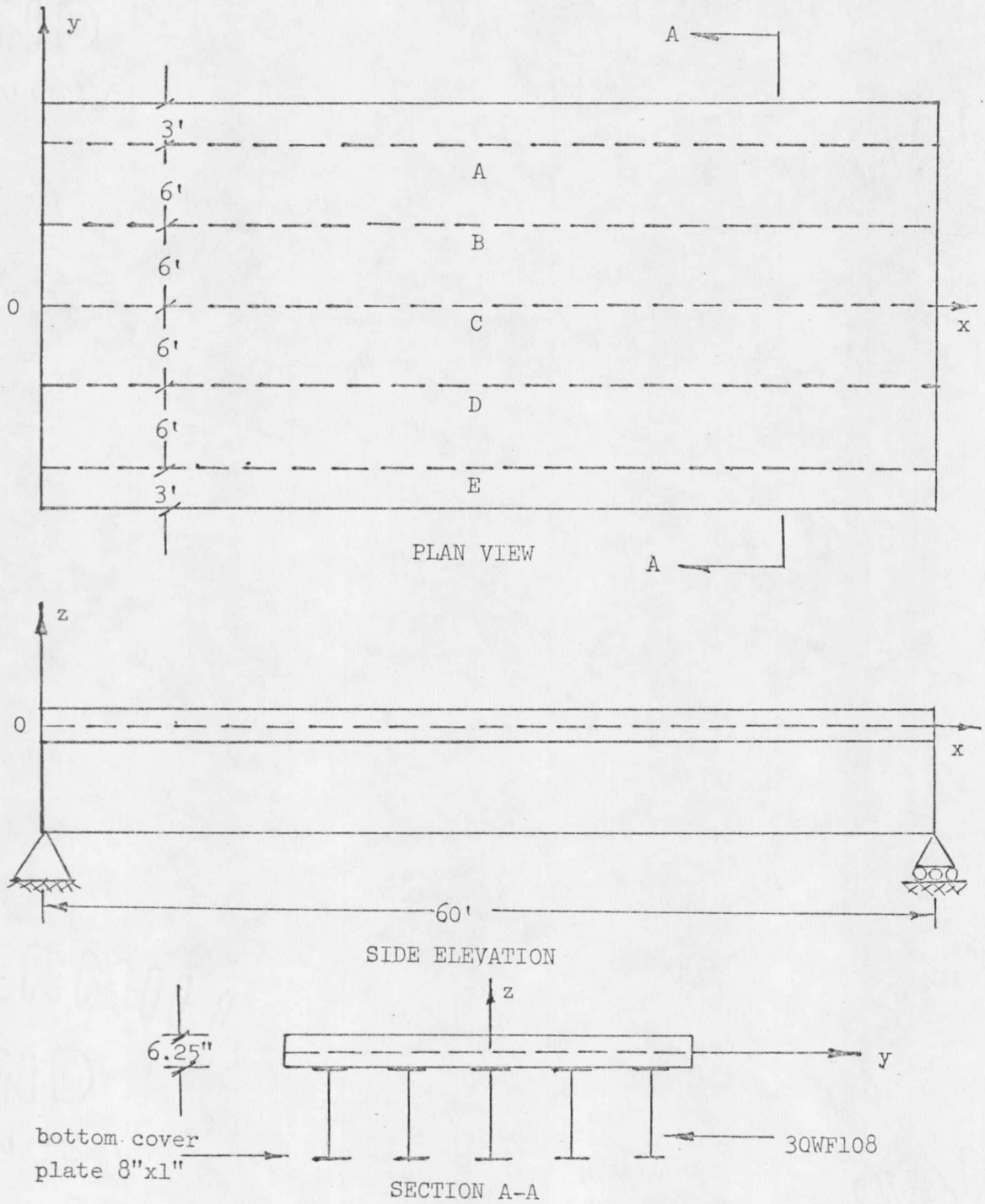


Figure 6. Details of simply supported five girder bridge.

TABLE I. Comparison of Moment Coefficients $C_m$ for 60 foot Span Composite I-Beam Bridge.

| Load Position | Basis of Comparison * | Coefficient of Moment $C_m^{\#}$ Mid-Span Section of Beam A | B | C | D | E |
|---|---|---|---|---|---|---|
| Mid-Span A | 1 | 0.1754 | 0.0872 | 0.0089 | -0.0128 | -0.0085 |
| | 2 | 0.1961 | 0.0592 | 0.0085 | -0.0058 | -0.0066 |
| | 3 | 0.1818 | 0.0651 | 0.0191 | -0.0019 | -0.0141 |
| Mid-Span B | 1 | 0.0543 | 0.1324 | 0.0540 | 0.0139 | -0.0046 |
| | 2 | 0.0598 | 0.1255 | 0.0536 | 0.0163 | -0.0051 |
| | 3 | 0.0636 | 0.1194 | 0.0510 | 0.0169 | -0.0010 |
| Mid-Span C | 1 | 0.0097 | 0.0539 | 0.1228 | 0.0539 | 0.0097 |
| | 2 | 0.0090 | 0.0540 | 0.1238 | 0.0540 | 0.0090 |
| | 3 | 0.0185 | 0.0512 | 0.1105 | 0.0512 | 0.0185 |
| 1/4-Span A | 3 | 0.0759 | 0.0447 | 0.0171 | -0.0005 | -0.0123 |
| 1/4-Span B | 3 | 0.0436 | 0.0377 | 0.0305 | 0.0129 | 0.0002 |
| 1/4-Span C | 3 | 0.0165 | 0.0306 | 0.0307 | 0.0306 | 0.0165 |
| 3/4-Span A | 3 | 0.0795 | 0.0431 | 0.0133 | -0.0018 | -0.0092 |
| 3/4-Span B | 3 | 0.0420 | 0.0388 | 0.0325 | 0.0129 | -0.0012 |

cont.

TABLE I. - Cont.

| Load Position | Basis of Comparison * | Coefficient of Moment $C_m$ for Quarter-Span Section of Beam A | B | C | D | E |
|---|---|---|---|---|---|---|
| Mid-Span A | 1 | 0.0709 | 0.0625 | 0.0067 | -0.0091 | -0.0060 |
| | 2 | 0.0875 | 0.0400 | 0.0066 | -0.0042 | 0.0047 |
| | 3(a) | 0.0647 | 0.0507 | 0.0271 | 0.0030 | -0.0205 |
| | 3(b) | 0.0817 | 0.0421 | 0.0112 | -0.0025 | -0.0074 |
| Mid-Span B | 1 | 0.0364 | 0.0463 | 0.0354 | 0.0102 | -0.0033 |
| | 2 | 0.0405 | 0.0412 | 0.0350 | 0.0122 | -0.0037 |
| | 3(a) | 0.0502 | 0.0303 | 0.0266 | 0.0149 | 0.0029 |
| | 3(b) | 0.0408 | 0.0401 | 0.0333 | 0.0126 | -0.0018 |
| Mid-Span C | 1 | 0.0072 | 0.0353 | 0.0400 | 0.0353 | 0.0072 |
| | 2 | 0.0070 | 0.0352 | 0.0408 | 0.0352 | 0.0070 |
| | 3(a) | 0.0267 | 0.0266 | 0.0184 | 0.0266 | 0.0267 |
| | 3(b) | 0.0108 | 0.0334 | 0.0367 | 0.0334 | 0.0108 |
| 1/4-Span A | 3(a) | 0.1311 | 0.0505 | 0.0224 | 0.0020 | -0.0185 |
| | 3(b) | 0.0351 | 0.0243 | 0.0099 | -0.0005 | -0.0063 |
| 1/4-Span B | 3(a) | 0.0498 | 0.0920 | 0.0317 | 0.0119 | 0.0021 |
| | 3(b) | 0.0235 | 0.0152 | 0.0152 | 0.0087 | -0.0001 |
| 1/4-Span C | 3(a) | 0.0222 | 0.0317 | 0.0798 | 0.0317 | 0.0222 |
| | 3(b) | 0.0096 | 0.0152 | 0.0128 | 0.0152 | 0.0096 |
| 3/4-Span A | 3(a) | 0.0267 | 0.0283 | 0.0178 | 0.0025 | -0.0128 |
| | 3(b) | 0.1502 | 0.0393 | 0.0056 | -0.0027 | -0.0048 |
| 3/4-Span B | 3(a) | 0.0281 | 0.0107 | 0.0119 | 0.0096 | 0.0022 |
| | 3(b) | 0.0378 | 0.1063 | 0.0375 | 0.0078 | -0.0020 |

# Moment = $C_m$ x Load x Span

* 1: Orthotropic plate theory (19)
2: Gustafson's model (46)
3: Present investigation
3(a): Moment coefficients at quarter-span
3(b): Moment coefficient at three-quarter-span

directly applied on these girders, are lower than the moments predicted by the orthotropic plate theory or Gustafson's finite element model. When the exterior girder A is loaded, the moment at the midspan of girder A is a little larger than the moment predicted by the orthotropic plate theory but is smaller than the moment given by Gustafson's model. This distribution of moments to the unloaded girders is similar in all the cases. The distribution of the load to the unloaded girders is a maximum when the central girder C is loaded, it is less when girder B is loaded and is a minimum when the exterior girder A is loaded. It is also observed that the moment coefficients at the quarter span of the loaded girders, computed by the present technique, are smaller than the corresponding coefficients predicted by Gustafson's model or the orthotropic plate theory. In Table I, the moment coefficients are also listed for three-quarter span section, with the quarter span moment coefficients. It is seen from these coefficients that the distribution of the moment along the span is not symmetric about the midsection of the bridge. The distribution of the moment coefficients is more uniform at the quarter spans than at the midspan when the loads are applied at the midsection of the various longitudinal girders.

The differences between the finite element model of Gustafson and the present model may be attributed to the lack of three dimensional nature of the Gustafson's model. Gustafson has treated the longitudinal girders as an assemblage of beam elements whose nodes coincide with the middle plane of the slab. In other words, the longitudinal girders are

assumed to stiffen the edges of the slab elements, and the entire bridge lies in one horizontal plane. Hence, when the vertical loads are applied, the model will not have reactions in the horizontal plane. The three dimensional model is found to have rather significant transverse and longitudinal reactions (Table VII). Similarly, the space-type behavior of the bridge leads to a different distribution of the vertical reactions at the two ends of the bridge. Since the horizontal reactions occur at the bottom plane, they will affect the moments. The moments in the various girders will be modified roughly in proportion to the magnitude and the elevation of the longitudinal reactions.

The differences with the orthotropic plate are attributed to two reasons: (1) the entire plate is in one plane as is the case with Gustafson's model, (2) the orthotropic plate model is obtained by smearing stiffness of the girders to obtain an equivalent plate model. It may be noted that the flexural and torsional rigidities of the equivalent orthotropic plates are obtained in an approximate manner, and the method is justifiable only if the longitudinal stiffeners are spaced so that the ratios of the stiffener spacing to the width of the bridge cross section are very small. Besides, the orthotropic plate theory ignores the stresses associated with the warping of the cross section which may be induced due to nonuniform distribution of the vertical loads.

The second bridge compared is a four-girder composite I-beam bridge (Figure 7). The bridge is 400 inches wide and is simply

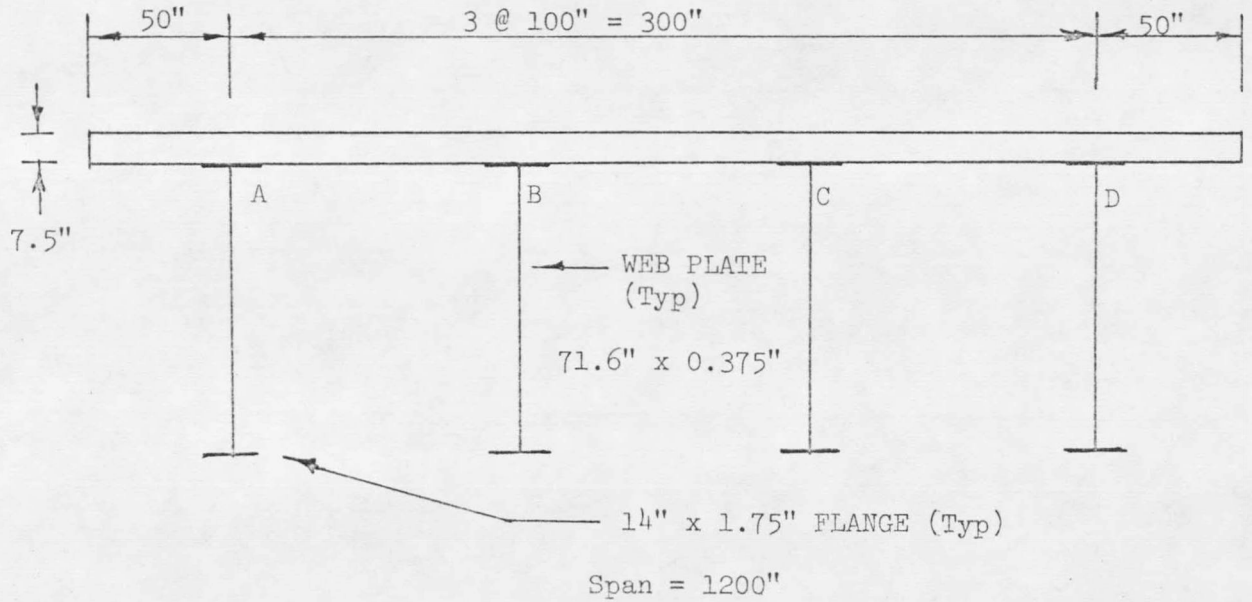


Figure 7. Details of 100' span composite I-beam bridge.

supported over a span of 1200 inches. The web plates of the longitudinal girders are 71.6" x 0.375" and the top and bottom flanges of the girders are 14.0" x 1.75". The bridge is analyzed for a line load of magnitude $\sin \frac{\pi x}{L}$; along an exterior girder A for one loading and along an interior girder B for the other loading.

The equivalent nodal forces for the sine loads are obtained by assuming that the deflected shape of the edge of the loaded girder can be represented by third order polynomials between the nodes of the elements. Alternately, it is assumed that the slab and the girder plate elements are compatible along their common edge, and the transverse displacement of the edge between two nodes is described by a third order polynomial.

The results of the analysis are compared in Table II with the results of Wright* and Gustafson. Wright's results are based on the direct stiffness method following the general assumptions described in Vlasov (47) for thin walled beam analysis. The structure is assumed to be an assemblage of plate elements which run the entire length of the structure from support to support.

The transverse slab moments $M_x$ per unit length of the slab and the longitudinal forces $N_x$ per unit width of the slab compare extremely well between Gustafson's finite element model and Wright's thin beam approach. However, these values are consistently higher in comparison to the present investigation, i.e., the present model results in smaller stresses in the slab.

* The results are obtained from Gustafson's thesis (46).

TABLE II. Comparison of Internal Forces for a Composite I-Beam Bridge (Figure 7).

1. Sine load acting on external girder A

| Force | Location x= | Basis of Comparison | Transverse Location A | B | C | D |
|---|---|---|---|---|---|---|
| $M_x$ in lbs/in Transverse slab moment per unit length (tension at bottom is +ve) | 0.50L | Wright* | 2.10 | -17.37 | -9.70 | -0.56 |
| | | Gustafson | 2.06 | -16.76 | -9.14 | -0.52 |
| | | Present | 1.69 | -12.37 | -5.07 | -0.51 |
| | 0.25L | Wright | 1.48 | -12.28 | -6.89 | -0.39 |
| | | Gustafson | 1.46 | -11.86 | -6.49 | -0.37 |
| | | Present | 0.83 | -7.07 | -2.59 | 0.55 |
| $N_x$ = lbs/in force in slab per unit width (tension + ve) | 0.50L | Wright | -13.11 | -7.49 | -2.21 | 2.78 |
| | | Gustafson | -13.63 | -7.87 | -2.37 | 2.84 |
| | | Present | -10.17 | -5.69 | -1.58 | -2.20 |
| | 0.25L | Wright | -9.28 | -5.31 | -1.56 | 1.96 |
| | | Gustafson | -9.66 | -5.54 | -1.64 | 1.98 |
| | | Present | -7.26 | -3.96 | -1.05 | 1.57 |

2. Sine load acting on internal girder B

| Force | Location x= | Basis of Comparison | Transverse Location A | B | C | D |
|---|---|---|---|---|---|---|
| $M_x$ Transyerse slab moment per unit length | 0.50L | Wright | -0.64 | 27.25 | -0.14 | -0.90 |
| | | Gustafson | -0.61 | 26.92 | -0.30 | -0.85 |
| | | Present | -0.51 | 21.40 | 3.34 | -0.61 |
| | 0.25L | Wright | -0.45 | 19.22 | -0.10 | -0.64 |
| | | Gustafson | -0.43 | 19.06 | -0.20 | -0.60 |
| | | Present | 0.01 | 12.48 | -2.34 | -0.25 |
| $N_x$ Force in slab per unit width | 0.50L | Wright | -7.54 | -6.11 | -4.23 | -2.18 |
| | | Gustafson | -7.82 | -6.39 | -4.45 | -2.29 |
| | | Present | -5.64 | -4.73 | -3.24 | -1.32 |
| | 0.25L | Wright | -5.33 | -4.32 | -2.99 | -1.54 |
| | | Gustafson | -5.49 | -4.56 | -3.19 | -1.58 |
| | | Present | -3.92 | -3.44 | -2.32 | -1.02 |

* The results are obtained from Gustafson's thesis.

In Wright's approach, any load between the simple supports of the bridge has to be represented by a series of sine loads acting along the edges of the plate elements. If the supports were not simple supports then the application of the method to the bridge problem would be extremely cumbersome. The ease of the finite element approach in treating various boundary conditions and loads is the prime advantage of the method.

A final comparison is made with the eighty foot span, four girder bridge of Figure 8. The bridge is analyzed without diaphragms in one case and with diaphragms spaced at an interval of quarter-span and at the end sections in the other case.

The results of the analysis are presented in Tables III, IV, and V along with Gustafson's results. The girder reactions $R_z$ for the case when the diaphragms are provided are read from Gustafson's plots. Figures 9 and 10 are plotted to indicate the influence of the diaphragms in distributing vertical loads to various unloaded girders.

The influence line coefficients $C_m$, for midspan girder moments in the present analysis has a distribution similar to Gustafson's solution. Here, it may be noted that the present analysis gives larger moments for the loaded girders than the finite element analysis of Gustafson. This distribution is in contradiction to the observation made during the comparison of five girder bridge of Figure 6. Here, the present method of analysis has resulted in smaller moment coefficients than Gustafson's computations (Table V).

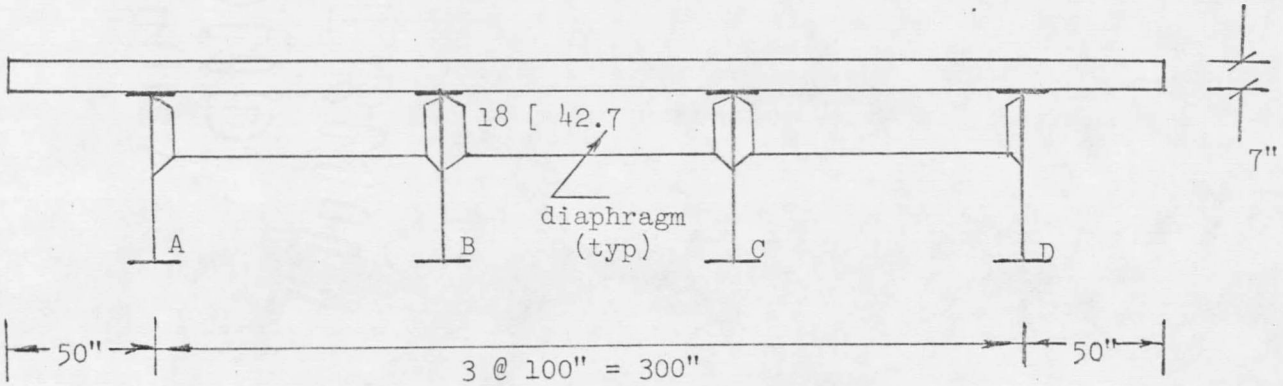


Bridge Cross Section

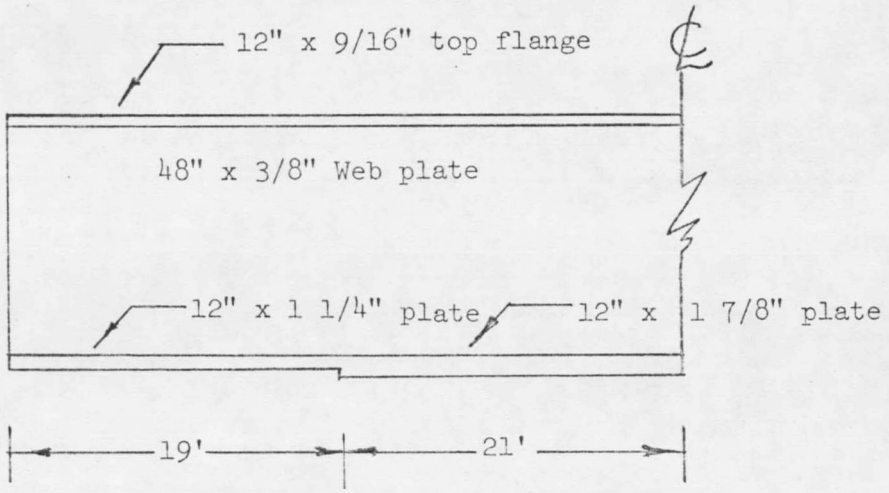


Typical Girder Elevation

Figure 8. 80' span, four girder bridge details.

TABLE III. Influence Coefficient $C_m$ for Mid-span Girder Moments for an 80' Span, Four Girder Bridge.

| Mid-span transverse load location | Girder | Without Diaphragms | | With Diaphragms | |
|---|---|---|---|---|---|
| | | Gustafson | Present Analysis | Gustafson* | Present Analysis |
| A | A | .1944 | .1996 | .1828 | .1866 |
| | B | .0621 | .0600 | .0754 | .0763 |
| | C | .0077 | .0068 | .0154 | .0135 |
| | D | -.0166 | -.0165 | -.0262 | -.0264 |
| B | A | .0621 | .0604 | .0763 | .0761 |
| | B | .1243 | .1311 | .1027 | .1041 |
| | C | .0533 | .0511 | .0533 | .0564 |
| | D | .0079 | .0075 | .0156 | .0134 |

* Diaphragms are treated as beam elements with their nodes at the middle plane of the slab.

TABLE IV. Influence Coefficients for Girder Reactions $R_z$ for an 80' Span Four Girder Bridge with Midspan Loadings

| Girder | Transverse Load Location | Gustafson | | Present Analysis | | | |
|---|---|---|---|---|---|---|---|
| | | No Diaph. | With Diaph. | No Diaphragms X=0* | No Diaphragms X=L** | With Diaphragms X=0 | With Diaphragms X=L |
| A | A | .3764 | .3380 | .4634 | .4015 | .3930 | .3614 |
| | B | .1582 | .1940 | .0910 | .1569 | .1663 | .1967 |
| | C | .0082 | .0450 | -.0400 | .0015 | .0105 | .0374 |
| | D | -.0401 | -.0120 | -.0073 | -.0560 | -.0696 | -.0945 |
| B | A | .1513 | .1890 | .0698 | .1372 | .1483 | .1788 |
| | B | .1711 | .1360 | .2792 | .1865 | .1791 | .1427 |
| | C | .1576 | .1280 | .1699 | .1551 | .1441 | .1233 |
| | D | .0144 | .0460 | -.0260 | .0173 | .0283 | .0543 |

* U, V, W are prevented (pinned)
** V, W are prevented (roller)

TABLE V. Influence Coefficient for the Vertical Reactions for an 80' Span Four Girder Bridge with Quarter Span Loadings

| Girder | Transverse Load Location | Gustafson | Present Analysis | | | | | | | |
|---|---|---|---|---|---|---|---|---|---|---|
| | | | Load at x = 19' | | | | Load at x = 61' | | | |
| | | No Diaph.* | No Diaph. | | With Diaph. | | No Diaph. | | With Diaph. | |
| | | | x=0# | x=L$ | x=0 | x=L | x=0 | x=L | x=0 | x=L |
| A | A | .6335 | .7464 | .1757 | .6734 | .1633 | .2111 | .6778 | .1740 | .6197 |
| | B | .1513 | .0595 | .0921 | .1557 | .1018 | .0588 | .1445 | .0937 | .2168 |
| | C | -.0062 | -.0449 | .0123 | -.0263 | .0270 | -.0178 | -.0176 | .0173 | .0080 |
| | D | -.0288 | .0079 | -.0406 | -.0405 | -.0541 | -.0106 | -.0380 | -.0473 | -.0815 |
| B | A | .1461 | .0428 | .0803 | .1406 | .0915 | .0457 | .1281 | .0828 | .2009 |
| | B | .4208 | .6000 | .0641 | .4260 | .0597 | .1022 | .4556 | .0682 | .3361 |
| | C | .1760 | .1479 | .0689 | .2071 | .0489 | .0941 | .1800 | .0584 | .2016 |
| | D | -.0016 | -.0346 | .0220 | -.0011 | .0368 | -.0087 | -.0053 | .0279 | .0234 |

* Load at quarter span
\# pinned end
$ roller end

It is interesting to note that the vertical reactions $R_z$ are not equal at both ends of the girders when the load is applied at the midspan. Similarly, we observe that the reactions $R_z$, at the pinned support at x=0 is not equal to the reactions $R_z$ at the roller support at x=L when the loads are applied at corresponding points. Obviously, the phenomenon is the result of the nonsymmetric boundary conditions of the bridge and the depth of the bridge girders which is properly considered in this analysis.

From Figures 9 and 10, considerable redistribution of the load is noted when the interior girder B is loaded. Whereas, when the exterior girder A is loaded, the distribution of load to the unloaded girders is skimpy. Inclusion of diaphragms in the bridge relieves the loaded girders. The change in the load carried by the loaded interior girder B is larger than the loaded exterior girder A.

From Figure 10, it may be observed that due to the presence of the diaphragms the reactions $R_z$ at the pinned end of the interior girder B is almost the same for the load on the exterior girder A and for the load on the interior girders B and C. Similarly, in Table IV the reactions $R_z$ at the roller end (x=L) of the girder B is seen to be greater when the load is applied on the exterior girder A than when the load is applied on the interior girder B itself. This clearly is due to greater redistribution of the load to the unloaded exterior girders, which occurs in the presence of the diaphragms.

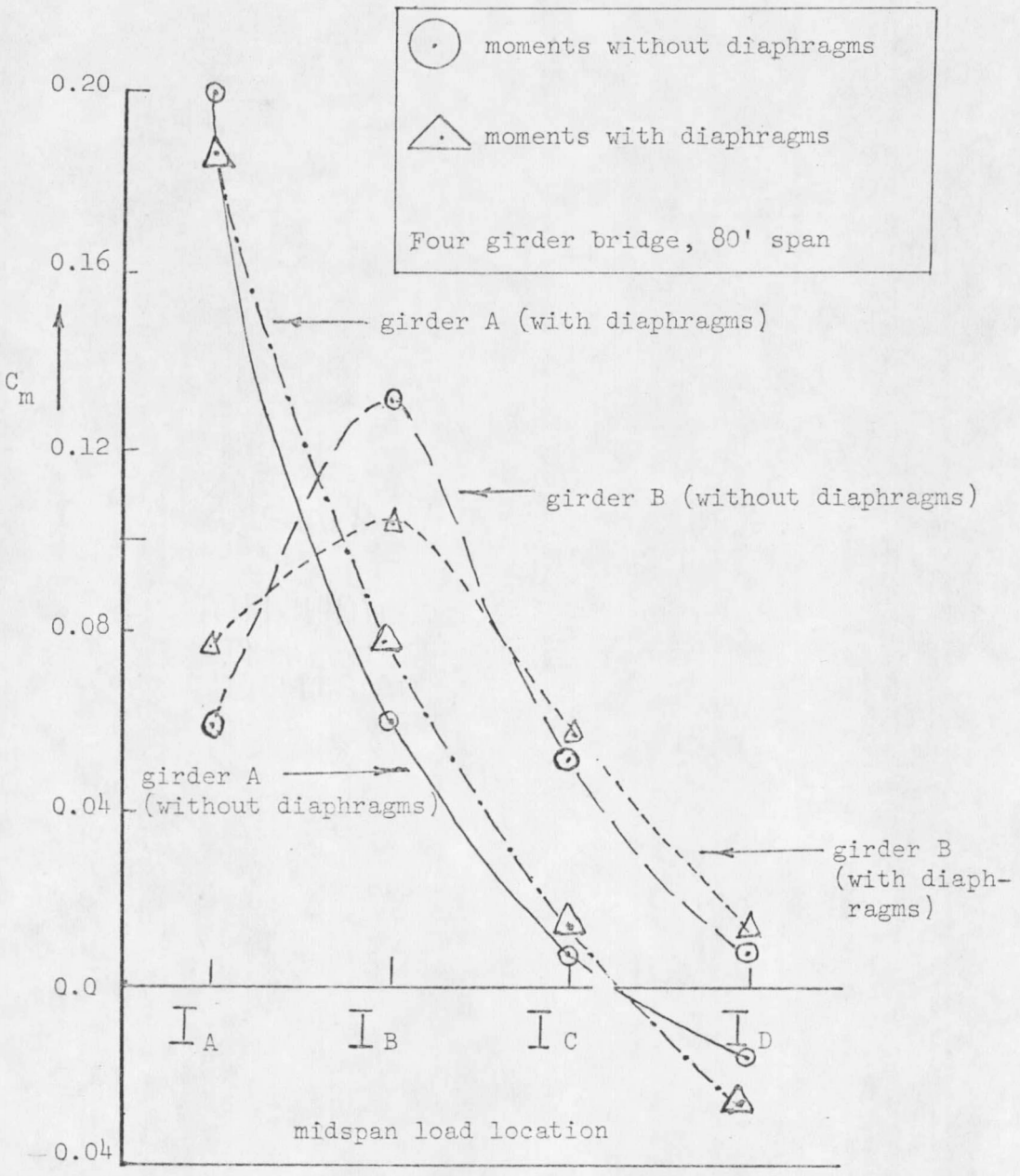


Influence lines for longitudinal moments of midspan of girders A and B.

Figure 9. Effect of diaphragms on composite girder moments.